JRC Scientific and Technical Reports

# Analysis of the Geometric Quality of the LPIS-based RapidEye level 3A

**Joanna Krystyna Nowak Da Costa**
**Piotr Andrzej Tokarczyk**

EUR 24132 EN - 2009

JRC
EUROPEAN COMMISSION

ipsc
Institute for the Protection and Security of the Citizen

The mission of the JRC-IPSC is to provide research results and to support EU policy-makers in their effort towards global security and towards protection of European citizens from accidents, deliberate attacks, fraud and illegal actions against EU policies.

European Commission
Joint Research Centre
Institute for the Protection and Security of the Citizen

**Contact information**
Address: T.P. 266, Via E. Fermi 2749, I-21027 Ispra (VA), Italy
E-mail: joanna.nowak@jrc.ec.europa.eu
Tel.: +39 0332 78 5854
Fax: +39 0332 78 9029

http://ipsc.jrc.ec.europa.eu/
http://www.jrc.ec.europa.eu/



JRC 56253

EUR 24132 EN
ISBN 978-92-79-14625-1
ISSN 1018-5593
DOI 10.2788/52547

Luxembourg: Office for Official Publications of the European Communities



*Printed in Italy*

## Table of Contents

## 1. Objective

This report summarizes the outcomes of the preliminary geometric image quality analysis of the LPIS-based (*) RapidEye level 3A image products. The objective of this study is twofold:

(1) to evaluate the planimetric accuracy of this product, in particular in the context of its suitability for the Common Agriculture Policy (CAP) Control with Remote Sensing (CwRS) Programme;

(2) to analyse the claim of the EFTAS company concerning the quality of the product.

(*) In this report we introduced the name 'LPIS-based RapidEye level 3A image product' to describe the RE product that is the result of the methodology for the standard RE level 3A product where the ground control points derived from the Global Landsat Mosaic are substituted for the ground control points derived from the LPIS vector data.

## 2. Acknowledgements

The authors would like to thank the EFTAS[1] company personnel, and in particular Jörn Brockmann and Robert Stein, who kindly provided us with their external quality control results and the set of their check points.

We also would like to thank the RapidEye[2] personnel, and in particular Scott Douglass, who kindly provided us with RE test data and technical assistance.

[1] EFTAS Fernerkundung Technologietransfer GmbH, Oststraße 2-18, 48145 Münster, Germany.

[2] RapidEye AG, Molkenmarkt 30, 14776 Brandenburg an der Havel, Germany.

## 3. Problem Description

The RapidEye (RE) system collects data at 6.5 meter nominal ground resolution and its ortho (level 3A) product can meet an accuracy of 6m 1-sigma (12.7m CE90[3]) with appropriate ground control ('RapidEye Standard Image Product Specifications', 2009). It corresponds to one-dimensional RMSE[4] of 6.5m.

The RapidEye standard image products are accepted as the high resolution (HR) sensors for the Common Agriculture Policy (CAP) Control with Remote Sensing (CwRS) Programme in 2009 Campaign. The 'Common Technical Specifications for 2009 Campaign of Remote Sensing control of area-based subsidies' preliminary describes the maximum 1-D RMSE value allowed for the RapidEye products as 11m.

According to the preliminary geometric quality analysis of the RapidEye image products (Nowak, 2009), this CwRS Orthoimagery Requirement for RapidEye image products is fulfilled for both standard 2A and 3A products, provided shift elimination based on the set of minimum 6 well-distributed ground control points. After this simple mathematic operation their 1-D RMSE can reach 2-3m[5], while the original 1-D RMS errors are 21.3m and 16.4m[6], respectively for East and North directions.

Provision of the more accurate auxiliary data to RapidEye should improve the geometric quality of the final image product. The LPIS[7] vector data can be treated as a source of the ground control points (GCPs) of better accuracy than the standard RapidEye auxiliary data, therefore, it was decided to test RE ortho product based on the GCPs derived from the LPIS vector data over two of the German 2009 CwRS zones, namely MFRA and WEIL.

Geometric quality analysis of this LPIS-based product requires the external quality control (EQC) based on the set of the independent check points. The EQC of the LPIS-based RE level 3A image product over MFRA and WEIL test site was initially performed by the EFTAS company, i.e. the German contractor for the CAP CwRS Programme in Germany.

1) It had been agreed that the final RE orthoimage level 3A based on the German LPIS data over MFRA test site ortho would be provided in the Gauss-Krueger Projection zone 4 (EPSG code 31494)[8]; RapidEye, however, provided product in their default projection, i.e. UTM WGS84.
2) The EFTAS company reprojected, by themselves, the delivered orthoimages into Gauss-Krueger 4 Projection, and then performed the external quality control (EQC) using check points chosen from their LPIS vector data. The EFTAS company made a complaint about the large RMS errors for this RE product, i.e. RMSE_X[9] of 5.17m and RMSE_Y of 8.58m.

---

[3] Horizontal accuracy (represented as CE90) is a horizontal measurement on the ground defining the radius of a circle within which an object of known coordinates should be found on an image. The probability of a point in the image meeting the recorded accuracy is 90% for CE90. This parameter is expressed in meters.

[4] Root Mean Square Error, the square root of the mean of the sum of the squares of the error residuals

[5] Based on the limited RapidEye sample images provided to EC JRC CID.

[6] for the analysed RapidEye 3A products

[7] Land Parcel Identification System (LPIS) is used for registration of agricultural reference parcels considered eligible for annual payments of European Common Agricultural Policy (CAP) subsidies to farmers.

[8] Coordinate Reference System code according to the European Petroleum Survey Group (EPSG)

[9] In this report, following the Gauss-Krueger coordinate system definition, X direction represents the easting, i.e. the projected distance of the position from the central meridian, while Y represents the northing, i.e. the projected distance of the point from the equator.

3) The EFTAS claim is based on their comparison between the results of the external quality control for two German test zones, i.e. WEIL and MFRA. The EFTAS EQC results of the WEIL test site are as follows: RMSE_X of 1.83m and RMSE_Y of 1.81m.

4) EFTAS also pointed out the differences of two pixels or more between the position of the LPIS parcels on the RE orthoimages and the LPIS vector data over MFRA site[10].

In order to understand the source of the differences in the EQC results and properly evaluate the geometric characteristics of the LPIS-based RE level 3A product, a comprehensive examination of the planimetric accuracy, including independent[11] external quality control, was performed.

[10] EFTAS visual inspection comments.

[11] By means of different software, different operator, and slightly different methodology

# 4. Data Description

## 4.1. Study Areas and Image Data

Our image test data consists of nine tiles (scenes) of the LPIS-based RapidEye level 3A product for two different test sites, as follows:

- three tiles overlapping in the North-South direction, and covering the WEIL study area situated in west Germany (Fig. 1).
- six tiles overlapping in both directions, acquired over the MFRA study area situated in central Germany (Fig. 2).

The LPIS-based RE level 3A product is radiometric, sensor and geometrically corrected and aligned to a cartographic map projection orthoimage. It is the RE Standard Ortho (level 3A) product, except the fact that the LPIS vector data served as a source of the ground control points instead of the Global Landsat Mosaic (standard RE auxiliary data).

The RE Standard Ortho (level 3A) product is delivered in Universal Transverse Mercator (UTM) projection and WGS84 horizontal datum, while the LPIS-based RapidEye level 3A product over MFRA and WEIL test sites is customised[12] to be provided in the Gauss-Krueger Projection zone 4 (EPSG code 31494)[13] and Gauss-Krueger Projection zone 2 (EPSG code 31492), respectively.

## 4.2. Validation Data

Two sets of ground control points (GCPs) served as the validation sets[14] in order to evaluate planimetric error of the test orthoimage data. EFTAS created this point datasets based on the LPIS vector data over the two CwRS test zones, i.e. MFRA and WEIL:

- MFRA_ICPs - set of 25 check points chosen from the German LPIS vector data over MFRA test site (Fig. 3) delivered in Gauss-Krueger Projection 4
- WEIL_ICPs - set of 25 check points chosen from the German LPIS vector data over WEIL zone (Fig. 4) delivered in Gauss-Krueger Projection 2.

[12] in accord with the EFTAS requirements.

[13] In the EPSG catalogue, the code 31494 stays for “DHDN/Germany Zone 4”.

[14] also referred as to independent control points (ICPs)

## 5. Methodology

The EU standard for the orthoimagery to be used for the purpose of the Common Agriculture Policy (CAP) Control with Remote Sensing (CwRS) requires the quality assessment of the final orthoimage ('Guidelines …,' 2008).

Geometric characteristics of the orthoimage product can be evaluated by performing the external quality control (EQC) that is comparing planimetric coordinates of well-defined and well-distributed points that were not included in the ortho-correction process with coordinates of the same points from an independent source of higher accuracy[15]. The RMS error calculated for the set of the independent control points in each dimension (either Easting or Northing) is used to describe the required product accuracy.

The main objective of this study was to analyse the geometric quality of the RE LPIS-based level 3A product, in particular its planimetric accuracy. The test data consists of nine orthoimages situated in two different CwRS test zones in Germany, MRFA and WEIL. These products are similar to the RE standard level 3A product, except for the fact that during the RE orthorectification process the standard RapidEye planimetric auxiliary data is replaced with set of ground control points derived from the LPIS vector data.

Quality evaluation of the set of image products implies their homogeneity, from both the statistics and good photogrammetric practice point of view. The EFTAS EQC results, i.e. the noticeably large differences between the RMSE values for MFRA and WEIL test sites, have motivated us to examine homogeneity of the LPIS-based RE level 3A product over MFRA and WEIL. Consequently, the accuracy assessment starts with studying data homogeneity.

In the second phase, we performed the external quality control and compare the quality values between the data of least unvaried characteristics. At this stage we also identified and eliminated the systematic shift by subtracting the average residual in both directions. Additionally, we tried evaluating the error of the check points' identification on the image test data since the quality of the validation data influence the external quality control results. Finally, we discuss the results and summarise key issues.

[15] These points are also referred to as independent control points (ICPs) or validation points.

# 6. Data Homogeneity Analysis

## 6.1. Test Data Production Workflow

The standard RE orthorectification process requires ground control points and terrain model to develop corrections for imagery distortions resulting from the RapidEye sensor viewing geometry. The RE auxiliary height data consists of the proprietary CGIAR-CSI[16] SRTM (90-m) dataset[17] and GTOPO30 (for areas above 60 degrees North). The ground control points are derived from the Global Landsat Mosaic. Typically around 5-7 GCPs are used per 25kmx25km RapidEye tile but some tiles are produced with as few as 2 points, therefore, the accuracy of the product varies from region to region based on available GCPs[18].

For the production of the LPIS-based RapidEye 3A product, the ground control points are derived from the LPIS vector data by their automatic identification on both: German LPIS and RE image data. As many as 90 GCPs from the LPIS data were used to generate the LPIS-based RE Ortho products over each test site, while the source of the height information remained the same (standard RE DEM).

Following requirements, the LPIS-based RapidEye level 3A product is customised[19] to be provided in the Gauss-Krueger Projection zone 4 (EPSG code 31494)[20] and Gauss-Krueger Projection zone 2 (EPSG code 31492), respectively for MFRA and WEIL test sites.

To sum up, there are three main differences that distinguish the LPIS-based RE level 3A product from the standard one (standard RE Ortho product):

- the quality, number and distribution of the GCPs,
- the resampling processes,
- the cartographic projection and coordinate system.

## 6.2. Quality, Number and Distribution of the GCPs

The worldwide RapidEye Ground Control Point database mainly includes points derived from the Landsat mosaic which positional accuracy is described as less then 50m (Tucker et al., 2004).

In case of the LPIS-based RE level 3A product, the Land Parcel Identification System (LPIS) data, a part of the Integrated Administrative and Control System (IACS) for Agricultural subsidies, established on the basis of maps or land registry documents or spatial imagery guaranteeing accuracy at least equivalent to maps of a scale of 1:10000 (article 20 of the Council Regulation (EC) No 1782/2003 of 29 September 2003) is used as a source of GCPs.

This scale accuracy requirement corresponds to the following minimum requirement of geometric accuracy for ortho-imagery and maps: one-dimensional root mean square error (1-D RMSE) of

[16] Consultative Group for International Agriculture Research Consortium for Spatial Information (http://srtm.csi.cgiar.org/).

[17] SRTM meet the absolute horizontal and vertical accuracies of 20 meters (circular error at 90% confidence) and 16 meters (linear error at 90% confidence), respectively (Rodriguez et al., 2005).

[18] For detailed technical information about RapidEye's Standard Image Product, please refer to the RapidEye Standard Image Product Specifications at http://www.rapideye.de/

[19] in accord with the EFTAS requirements.

[20] In the EPSG catalogue, the code 31494 stays for “DHDN/Germany Zone 4”.

2.5m[21,22,23]. The LPIS-based RE level 3A product is, therefore, based on circa ten times more accurate ground control points.

Our test data consists of nine scenes of the LPIS-based RE level 3A product situated in two different test zones, i.e. MRFA and WEIL. Ninety LPIS ground control points were used to generate the LPIS-based RE Ortho products over each test site. Assuming that RapidEye assures equal distribution of GCPS over each scene, the number of GCPs is at least tripled in case of the LPIS-based level 3A product.

### 6.3. Resampling Processes

Resampling conducted in Cubic Convolution is a regular component of the RE standard orthorectification process, and the RE Standard Ortho (level 3A) product is delivered in Universal Transverse Mercator (UTM) projection and WGS84 horizontal datum. Fulfilment of the requirement for the LPIS-based RapidEye level 3A product over MFRA and WEIL test sites to be delivered in the Gauss-Krueger Projection is done at RE through reprojection using commercially available software (here: PCI Geomatica Focus standard reprojection tools). This process implies resampling and it is conducted in Nearest Neighbor method.

It is well known that lower order interpolation methods (eg. nearest neighbour) produce artifacts, while higher order interpolation methods tend to blur the image. Each data sampling influences image data. Double data interpolation most likely weakens perceptual image quality. This can badly affects the possibility of the point identification on image, and in consequence, image geometric accuracy.

### 6.4. Cartographic Projection and Coordinate System

As mentioned before, the MFRA and WEIL RapidEye Ortho tiles were reprojected from Universal Transverse Mercator (standard RE cartographic coordinate system) to the Gauss-Krueger Projection and Coordinate System.

These two coordinate systems are based on Transverse Mercator projection (cylindrical, conformal, where the projected surface is aligned to a central meridian), however:

- central meridians of the Gauss-Krueger zones are only 3° apart, as opposed to 6° in UTM;
- scale factor along the central meridian of the Gauss-Krueger is 1.0000 (and increases with distance from central meridian), as opposed to 0.9996 in UTM[24].
- Gauss-Krueger local linear scale factor increases with the longitude difference (between the central meridian and tested point), and with the latitude (the closer to the equator, the smaller distortion is).

The relationship between these two, well-know cartographic coordinate systems has curvilinear character, therefore the reprojection from UTM to Gauss-Krueger (or vice versa) should be done based on these systems mathematically rigorous formulas. In case of using the approximate

[21] ASPRS interim accuracy standards for large scale maps, 1989.

[22] Kay et al., 1997, Operational activities involving airborne remote sensing related to the Common Agricultural Policy, Proceedings of the 3rd International Airborne Remote Sensing Conference and Exhibition.

[23] Discussion document “Implementation of IACS-GIS, Reg.1782/03 and 796/2004”, JRC IPSC/G03/P/SKA/skaD (2004)(2575)..

[24] Distortion of scale increases to 1.0010 at the outer zone boundaries along the equator the overall distortion of scale inside the entire zone is minimized.

reprojection method, the conformal transformation of the second order would be the best choice, or at least affine transformation[25].

We do not have enough information about the reprojection methods that were used in case of MFRA and WEIL, however we are afraid that the EDRAS Imagine (used by EFTAS) and the PCI Geomatica (used by RapidEye) standard reprojection tools may not be enough sophisticated. We expect the significantly large distortions to appear, especially in case of MFRA orthos that are further form the central meridian and closer to the equator (Tab.1 and Fig.5).

| Test zone name | Product name (ID) | Across track incidence angle [deg] | Coordinate System and zone | Distance from the Gauss-Krueger central meridian [km] | |
|---|---|---|---|---|---|
| | | | | Max | Min |
| MFRA | 1136205_44574 (also referred as to MFRA2) | 5.7 | Gauss-Krueger 4 | 122 | 96 |
| | 1214946_44695 (also referred as to MFRA1) | 5.2 | | | |
| | 1136128_44574 (also referred as to MFRA0) | 4.7 | | | |
| | 1136203_44574 | 7.7 | | 98 | 72 |
| | 1136204_44574 | 7.2 | | | |
| | 1136202_44574 | 6.7 | | | |
| WEIL | 953044_38645 | 7.1 | Gauss-Krueger 2 | 70 | 42 |
| | 953000_38645 (also referred as to WEIL1) | 7.6 | | | |
| | 952855_38645 | 8.2 | | | |

**Table 1. The distance from the Gauss-Krueger central meridian and across track incidence angle for the WEIL and MFRA ortho tiles.**

### 6.5. Data Comparability

Quality evaluation of the set of image products implies their homogeneity, from both the statistics and good photogrammetric practice point of view. Data of varying characteristics should be treated separately, as regards its quality values.

**Are the LPIS-based RE level 3A tiles over MFRA and WEIL obtained in the same manner?**

IMAGE ACQUISITION

[25] or using Least Square Method adjustment.

- All test images present moderate across track incidence angles (Tab.1) typically selected for space mapping applications and they are similar in terms of acquisition characteristics and processed to same level.

IMAGE ORTHORECTIFICATION

- Auxiliary data quality is similar for both test sites, however, the height model, i.e. CGIAR-CSI SRTM data product[26], its influenced by systematic height errors (bias) depending on terrain relief and inclination (Passini and Jacobsen, 2007; Castel and Oettli, 2008). In general a lower accuracy in mountainous, hilly and/or covered by forest areas can be expected. And while WEIL test zone is almost flat, MFRA is characterized by hilly topography with 150-m elevation differences.
- Number and distribution of the points used for image correction may differ from image to image.

REPROJECTION

- MRFA and WEIL tiles are both reprojected into Gauss-Krueger Projection projection, however (a) the MFRA site is further from its central meridian and closer to the equator than WEIL site therefore the local scale differences should be taken into account, (b) transformation and resampling of the MFRA was done using two different procedures:
    - by EFTAS using ERDAS Imagine reprojection tool[27],
    - by RapidEye using PCI Geomatica Focus standard reprojection tool and Nearest Neighbor resampling method[28],

  introducing additional image distortions and changing perceptual image quality.

From above, one can notice the existence of the differences both in the ortho production phase and the reprojection phase. It should not be forgot during the comparison of the results of the external quality control of the LPIS-based RE level 3A tiles over MFRA and WEIL sites.

Additionally, we noticed that EFTAS treated all MFRA as a ‘block’ of images and calculated the RMS errors per block, however, during the standard RapidEye production workflow each RE Ortho tile is created independently (single scene processing). No block adjustment was involved nor for WEIL neither for MFRA RE scenes, therefore, their quality control needed to be performed separately.

[26] The final seamless dataset with voids filled in available in GeoTiff format at the website of Consultative Group for International Agriculture Research Consortium for Spatial Information (CGIAR-CSI) via http://srtm.csi.cgiar.org/.

[27] At the time of report writing, we haven’t got enough information about which method the resampling was conducted.

[28] This procedure is identical like the one used for WEIL LPIS-based RE 3A tiles.

# 7. Results

### 7.1. MFRA and WEIL external quality control by EFTAS

The EFTAS company examined following sets of the LPIS-based RE level 3A tiles:

- WEIL - 3 scenes overlapping in the North-South direction, reprojected by RapidEye to Gauss-Krueger Projection zone 2 (EPSG code 31492) using commercially available software (here: PCI Geomatica Focus standard reprojection tools), where the resampling was conducted in Nearest Neighbor method.
- MFRA - 6 scenes overlapping in both North-South and West-East directions, reprojected by EFTAS to Gauss-Krueger Projection zone 4 using ERDAS Imagine tools.

EFTAS performed the external quality control over MFRA and WEIL tiles and they obtain the following results (compare Appendix 3 and 4):

WEIL: RMSE_X (East) = 1.83m and RMSE_Y (North) = 1.81m

MFRA: RMSE_X (East) = 5.17m and RMSE_Y (North) = 8.58m

Note that EFTAS treated all MFRA tiles and all WEIL tiles as a block of images and calculated the RMS errors per block.

### 7.2. MFRA and WEIL external quality control by the JRC

We (CID Action from the EC JRC) examined following sets of the LPIS-based RE level 3A tiles:

- WEIL - 3 scenes overlapping in the North-South direction, reprojected by RapidEye to Gauss-Krueger Projection zone 2 (EPSG code 31492) using commercially available software (here: PCI Geomatica Focus standard reprojection tools), where the resampling was conducted in Nearest Neighbor method.
- MFRA - 6 scenes overlapping in both North-South and West-East directions, reprojected by RapidEye to Gauss-Krueger Projection zone 4 (EPSG code 31494) using commercially available software (here: PCI Geomatica Focus standard reprojection tools), where the resampling was conducted in Nearest Neighbor method.

We performed the external quality control over MFRA and WEIL tiles using the same validation data as EFTAS, however each tile was treated independently.

All points from WEIL_ICPs dataset covered one WEIL tile (2009-04-21T111505_RE3_3A-NAC_953000_38645_GK2) therefore we could perform the EQC on this tile only (Appendix 6):

WEIL1: RMSE_X (East) = 2.58m and RMSE_Y (North) = 2.73m

As far as the MFRA site is concerned, only two of six tiles (2009-06-13T110742_RE4_3A-NAC_1214946_44695_GK, 2009-06-13T110746_RE4_3A-NAC_1136205_44574_GK) were covered by significant[29] number of the check points from MFRA_ICPs dataset. We obtained the following one-dimensional root mean square errors (Appendix 5):

MFRA1: RMSE_X (East) = 2.68m and RMSE_Y (North) = 5.14m

MFRA2: RMSE_X (East) = 14.26m and RMSE_Y (North) = 9.62m

[29] In both cases we had eight check points.

### 7.3. Systematic Error Elimination

Analysing MFRA tiles, we noticed that the differences between validation (reference) coordinates and the measured coordinates show a significant systematic behaviour in the tile 2009-06-13T110746_RE4_3A-NAC_1136205_44574_GK (MFRA2, Fig. 6).

The systematic shift for each validated product can be found in the Table 2. The shift was determined and eliminated by subtracting the average residual.

| | | Average residual in X (East) direction [m] | Average residual in Y (North) direction [m] |
|---|---|---|---|
| WEIL1 | reprojected and measured by EFTAS | -0.36 | -0.25 |
| MFRA1 | reprojected and measured by EFTAS | 0.22 | -6.63 |
| MFRA2 | reprojected and measured by EFTAS | 1.25 | -9.39 |
| WEIL1 | reprojected by RE, measured by the JRC | 0.06 | 0.52 |
| MFRA1 | reprojected by RE, measured by the JRC | -0.35 | -0.23 |
| MFRA2 | reprojected by RE, measured by the JRC | 13.68 | -9.47 |

**Table 2: The systematic shift values determinated for the tested WEIL and MFRA LPIS-based Ortho tiles.**

### 7.4. Point Identification Error

The quality of the validation point data was evaluated by EFTAS and JRC.

EFTAS performed two independent point identifications (measurements) on the LPIS source data, therefore the point identification on LPIS data source was derived as the standard deviation based on two independent point measurements (see Appendix 7.1 for MFRA and 7.2 for WEIL).:

STD_LPIS_MRFA=0.07m

STD_LPIS_WEIL=0.10m

We (the JRC) obtained the point identification error on the RE image data source as the standard deviation calculated from the set of ten independent measurements of the chosen ICPs on the RapidEye image products:

STD_MFRA_RE= 1.48÷2.97m (see Appendix 1).

STD_WEIL_RE= 1.71÷5.49m (see Appendix 2).

# 8. Discussion

## 8.1. EQC Results Comparison

Each RapidEye product is orthorectified on a scene by scene basis. No block adjustments are made, therefore, the external quality control needed to be performed separately for each RE scene.

Based on the EFTAS results, we calculated the RMSE for the only three products that are covered by significant number of check points, thus we could compare results of their and our external quality control. The summary table shows one-dimensional root mean squares before and after systematic error elimination (Appendix 8).

It must be underlined that EFTAS and the JRC performed quality control on the same set of data but the reprojection was done using different procedures.

Note that by simple elimination of the systematic shift, the accuracy of the LPIS-based RE 3A product is comparable to the theoretical expected accuracy described in the RapidEye Product Specifications, i.e. 1-D RMSE of 6.5m, independently of the process or tools used for image reprojection.

## 8.2. Systematic Shift

During the standard RapidEye production workflow each RE Ortho tile is created independently, thus slight locational differences between tiles may occur.

One MFRA tile shows a significant systematic behaviour, with an average shift of 13.73m in Easting and -9.5m in Northing (tab.2). This may be explained by a bias in the SRTM in the RapidEye georeferencing and orthorectification process. Erroneous elevation values can lead to horizontal shift. While WEIL test zone is almost flat, MFRA is characterized by hilly topography with 150-m elevation differences.

Our comparison of the three MFRA tiles, overlying in South-North direction, showed some shift in pixel locations (Fig.8). Similar occurrence was also reported by EFTAS, therefore we measured this shift on 10 tie points chosen for this exercise. The results of shift measurements can be found in Appendix 9.1 and Appendix 9.2, while the average shift is presented on Fig. 7.

This identified and measured horizontal shift between the neighbouring orthoimages has similar value and direction as the above mentioned systematic shift, therefore we claim that it is the same shift.

The shift between the original, not reprojected to Gauss-Krueger tiles (see Appendix 9.1 and 9.2) has the same value and direction like this one observed on the reprojected tiles. This fact indicates that the shift appeared prior to reprojection process. The possible explanation is the heterogeneous SRTM quality.

## 8.3. Reprojection Influence

Reprojection of the RE Ortho tiles from its standard coordinate system and projection (UTM) to the requested one (Gauss-Krueger) using the off-the-shelf photogrammetric systems (i.e. ERDAS Imagine, PCI Geomatica):

- decreases the ability of GCP/ICP location in the imagery with high accuracy;
- introduces additional image distortions (by not taking into account the local scale changes in the Gauss-Krueger projection and coordinate system).

On the MFRA tiles reprojected using PCI Geomatica software, we observed a strange anomaly (Fig. 11) that degrades the geometric and radiometric image quality.

The RE orthoimages in UTM projection are not affected, as well as the image data reprojected by EFTAS using different software (Fig.12).

The standard deviation of the shift observed between the MFRA scenes (Appendix 10.1, 10.2) also seems to be higher for the orthoimages that were reprojected to Gauss-Krueger, however the reprojection influence on orthoimage quality needs further investigation.

### 8.4. Validation Data Quality

Geometric accuracy of orthoimage depends on many factors including the quality and suitability of the points used for image correction and product validation (Davis and Wang, 2003; Kay et al., 2003; Chmiel et al., 2004):

(a) the high horizontal/vertical positional accuracies of the GCP/ICP data (correction and validation data)

(b) a priori selection/identification of the GCP/ICP locations at sharp and distinct point features in the digital imagery (the more similar to the test image data the better)

(c) the ability of the software operator to select/identify the GCP/ICP location in the imagery with high accuracy.

Additionaly, check points used for orthoimage external quality control:

- must not be used during the image correction phase;
- should come from different measurement source than points used during orthorectification;
- should be characterised by accuracy at least 3 times more than the expected ortho-product accuracy (5-times recommended).

During the external quality control measurements we noticed that several ICPs were not well-defined and they were hardly identifiable on the test orthoimages, e.g. the points located on the border between two crop fields (Fig. 9). The validation points were chosen from the German LPIS vector data and their accuracy is influenced by several factors:

- MFRA ICPs - Set of 25 ground control points chosen from the German LPIS vector data over MFRA test zone (Fig. 3):
    - The accuracy of the LPIS data over the MFRA test zone is 0.60m[30]
    - Point identification on LPIS data source - the standard deviation based on two independent point identifications (measurements) [31] on the LPIS source data, STD_LPIS_MRFA=0.07m (see Appendix 7.1).
    - Point identification error on the RE image data source - the standard deviation calculated from the set of 10 independent measurements of the chosen GCPs on the RapidEye image products, 1-D STD_MFRA_RE= 1.48÷2.97m (see Appendix 1). Good estimation of the identification error on image data can be the as the square root of the smallest and the largest 1-D STD:

      ((1.48)^2 + (2.97)^2)^1/2 = 3.32m

  These accuracy components are independent therefore the final MFRA ICPs accuracy can be defined as the square root of the sum of squares of the independent error components:

  ((0.60)^2 + (0.07)^2+ (3.32)^2)^1/2 = (0.36 + 0.0049+ 11.02)^1/2 = 3.37m

[30] Information provided by the EFTAS company.

[31] Measured by the EFTAS company.

- WEIL ICPs - Set of 25 ground control points chosen from the German LPIS vector data over WEIL test zone (Fig. 4):
    - The accuracy of the LPIS data over the WEIL test zone is 0.45m[32]
    - Point identification on LPIS data source- the standard deviation based on two independent point identifications (measurements) on the LPIS source data, STD_LPIS_WEIL=0.10m (see Appendix 7.2).
    - Point identification error on the RE image data source - the standard deviation calculated from the set of 10 independent measurements of the chosen GCPs on the RapidEye image products, 1-D STD_WEIL_RE= 1.71÷5.49m (see Appendix 2). Good estimation of the identification error on image data can be the as the square root of the smallest and the largest 1-D STD:

      ((1.71)^2 + (5.49)^2)^1/2 = 5.75m

  These accuracy components are independent therefore the final WEIL ICPs accuracy can be defined as the square root of the sum of squares of the independent error components:

  ((0.45)^2 + (0.10)^2+ (5.75)^2)^1/2 = (0.2025 + 0.01+ 33.06)^1/2 = 5.77m

To sum up, the MFRA/WEIL point validation data source is the same like the one used for GCPs derivation, i.e. German LPIS vector data, many points are not located at sharp and distinct point features, and their accuracy is between 3.3m and 5.8m, therefore the validation data do not fulfil the quality and suitability requirements, especially if the expected final product accuracy is 6.5m (1-D RMSE).

[32] Information provided by the EFTAS company.

## 9. Summary of Key Issues

This report describes the geometric image quality of the LPIS-based RapidEye level 3A product in the context of the Common Agriculture Policy (CAP) Control with Remote Sensing (CwRS) Programme. This product is similar to the RE standard level 3A product, but the standard RapidEye planimetric auxiliary data is replaced with a set of ground control points derived from the LPIS vector data.

The key issues identified during the geometric quality analysis of the nine provided LPIS-based RE level 3A tiles (scenes) are summarised below:

- Each RapidEye product is orthorectified on a scene by scene basis, therefore, the external quality control must be performed separately for each RE scene.
- Three of nine LPIS-based RE level 3A tiles, namely WEIL1, MFRA1 and MFRA2, have a satisfactory number of check points, therefore, and they were the only tiles where independent quality control was performed.
- The provided validation data do not fulfil the quality and suitability requirements, if the expected final product accuracy is 6.5m (1-D RMSE).
- The comparison of the EQC demonstrates large differences between the RMSE values for MFRA and WEIL tiles and therefore the test data homogeneity was questioned.
- The tested image products are not homogeneous with respect to:
  - the quality, number and distribution of the GCPs – this influences the geometry characteristics of the orthorectification process result;
  - the relief and terrain inclination, i.e. the input height data (SRTM) accuracy – this can lead to horizontal shift on the ortho product;
  - the distance from the central meridian and equator – this influences the Gauss-Krueger projection's distortions and local scale values;
  - the transformation and resampling type – this influences the perceptual and geometric quality of the reprojection process product.

The above points should be taken into account while interpreting accuracy results of the final product.

Based on the current analysis there are two issues that most likely driving the differences in the geometric quality of the provided tiles: the heterogonous quality of the input height data and a low polynomial order for reprojection to the Gauss-Krueger. In order to comprehensively verify these hypotheses, the quality analysis must be repeated

(1) using the MFRA/WEIL RE orthoimages in the original RE projection and coordinate system (i.e. UTM). This action, however, requires the check points coordinates to be delivered in the UTM coordinate system or their reprojection based on the original rigorous mathematical formulas;

(2) using more RapidEye sample images. This action requires also the provision of the validation data over them.

**Based on the limited RapidEye sample images, the accuracy of the LPIS-based RapidEye level 3A products is within the RE product specifications accuracy (1-D RMSE of 6.5m) provided the shift elimination based on the set of well-distributed ground control points.**

## 10. References


- American Society for Photogrammetry and Remote Sensing (ASPRS), 1989. ASPRS interim accuracy standards for large scale line maps. Photogrammetric Engineering and Remote Sensing, 55, pp.1038-1040.
- Castel, T., Oettli, P., 2008. Sensitivity of the C-band SRTM DEM Vertical Accuracy to Terrain Characteristics and Spatial Resolution. In: Headway in Spatial Data Handling Lecture Notes in Geoinformation and Cartography, ISSN 1863-2246, Springer Berlin Heidelberg, ISBN 978-3-540-68565-4 (Print) 978-3-540-68566-1 (Online), Pages 163-176.
- Chmiel, J., Kay, S. and Spruyt, P., 2004. Orthorectification and geometric quality assessment of very high spatial resolution satellite imagery for Common Agricultural Policy purposes.. Proceedings of XXth International Archives of the Photogrammetry, Remote Sensing and Spatial Information Sciences, 35(Part B4), pp. 1-6. ISPRS, Istambul.
- Common Technical Specifications for the 2009 Campaign of Remote-Sensing Control of Area-Based Subsidies (ITT no. 2008/S 228-302473, JRC IPSC/G03/P/HKE/hke D(2008)(10021), Int. ref: file://S:\FMPArchive\P\10021.doc)
- Council Regulation (EC) No 1782/2003 of 29 September 2003 establishing common rules for direct support schemes under the common agricultural policy and establishing certain support schemes for farmers and amending Regulations (EEC) No 2019/93, (EC) No 1452/2001, (EC) No 1453/2001, (EC) No 1454/2001, (EC) 1868/94, (EC) No 1251/1999, (EC) No 1254/1999, (EC) No 1673/2000, (EEC) No 2358/71 and (EC) No 2529/2001; Official Journal L 270 , 21/10/2003 P. 0001 – 0069 (available on line at: http://eur-lex.europa.eu/LexUriServ/LexUriServ.do?uri=CELEX:32003R1782:EN:HTML )
- Davis, C.H., Wang, X., 2003. Planimetric accuracy of Ikonos 1 m panchromatic orthoimage products and their utility for local government GIS basemap applications. International Journal of Remote Sensing, Volume 24, Number 22, 2003 , pp. 4267-4288(22), Taylor and Francis Ltd.
- Discussion document “Implementation of IACS-GIS, Reg.1782/03 and 796/2004”, JRC IPSC/G03/P/SKA/skaD (2004)(2575).
- Kapnias, D., Milenov, P., Kay, S., 2008. ‘Guidelines for Best Practice and Quality Checking of Ortho Imagery’ Issue 3.0. EUR 23638 EN – 2008.
- Kay, S., Léo, O., Meyer Roux, J., Delincé, J, and Van de Steene, M., 1997. Operational activities involving airborne remote sensing related to the Common Agricultural Policy. Proceedings of the 3rd International Airborne Remote Sensing Conference and Exhibition, 7-10 July 1997, pp I-79-86.
- Kay, S., Spruyt, P. and Alexandrou, K., 2003. Geometric quality assessment of orthorectified VHR space image data. Photogrammetric Engineering and Remote Sensing, 69, pp. 484-491.
- Morris, A. C., Stevens, A., Muller J.-P. A. L., 2006. Ground Control Determination For Registration Of Satellite Imagery Using Digital Map Data. The Photogrammetric Record, Volume 12 Issue 72, Pages 809 – 822, Journal Compilation © 2009 Remote Sensing and Photogrammetry Society and Blackwell Publishing Ltd.

- Nowak Da Costa, J., 2009. RapidEye – Initial findings of Geometric Image Quality Analysis. JRC Scientific and Technical Report PUBSY no.56252, EUR 24129 EN, IPSC/G03/C/JN/ D(2009)(10879), Int. ref: file://S:\FMPArchive\C\10879.pdf
- Passini, R., Jacobsen, K., 2007. Accuracy Analysis of SRTM Height Models: ASPRS annual conference. Tampa, 2007.
- 'RapidEye Standard Image Product Specifications', August 2009 (http://www.rapideye.de/)
- Rodriguez, E., Morris, C. S., Belz, J. E., Chapin, E. C., Martin, J. M., Daffer, W., Hensley, S., 2005. An assessment of the SRTM topographic products. Jet Propulsion Laboratory D-31639.
- Toutin, Th., 2003. Error tracking in IKONOS geometric processing using a 3D parametric modelling. Photogrammetric Engineering and Remote Sensing, 69(1), 43-51.
- Tucker, C.J., Grant, D.M., Dykstra, J.D., 2004. NASA's Global Orthorectified Landsat Data Set. Photogrammetric Engineering & Remote Sensing Vol. 70, No. 3, March 2004, pp. 313–322. Journal of the American Society for Photogrammetry and Remote Sensing.

## 11. Figures

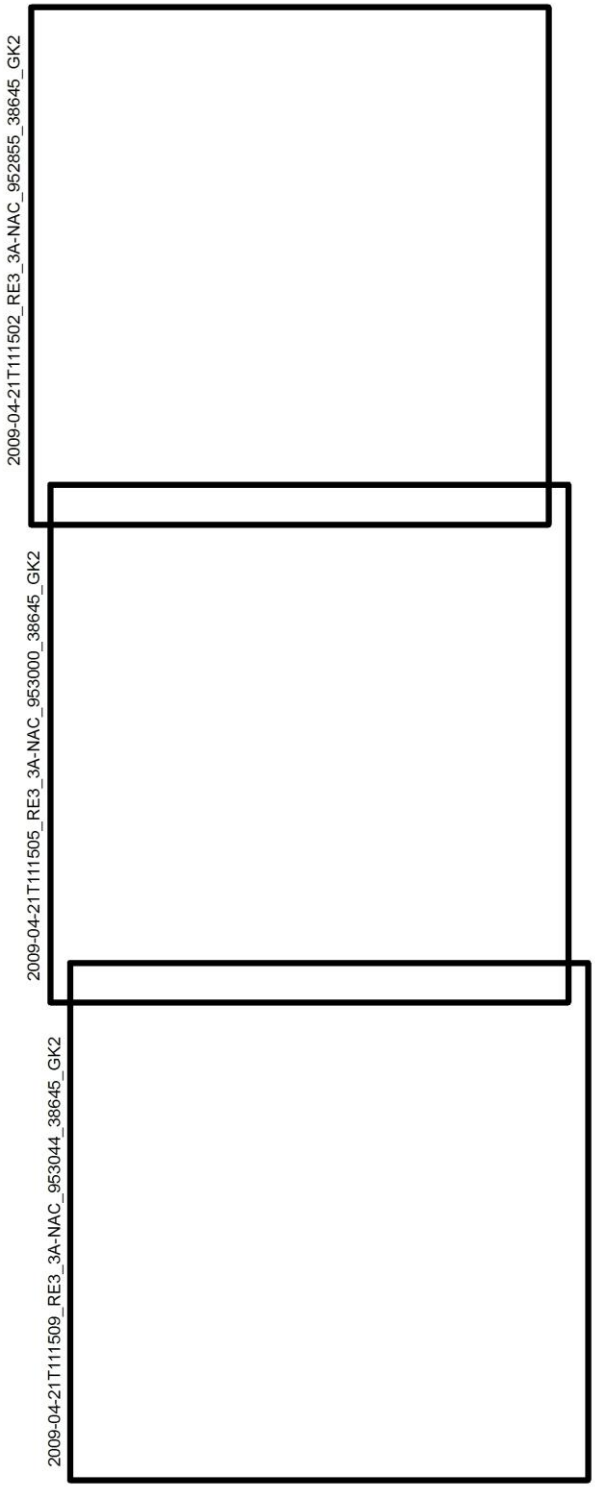


**Figure 1: Three RapidEye tiles overlapping in the North-South direction, and covering the WEIL study area situated in west Germany.**

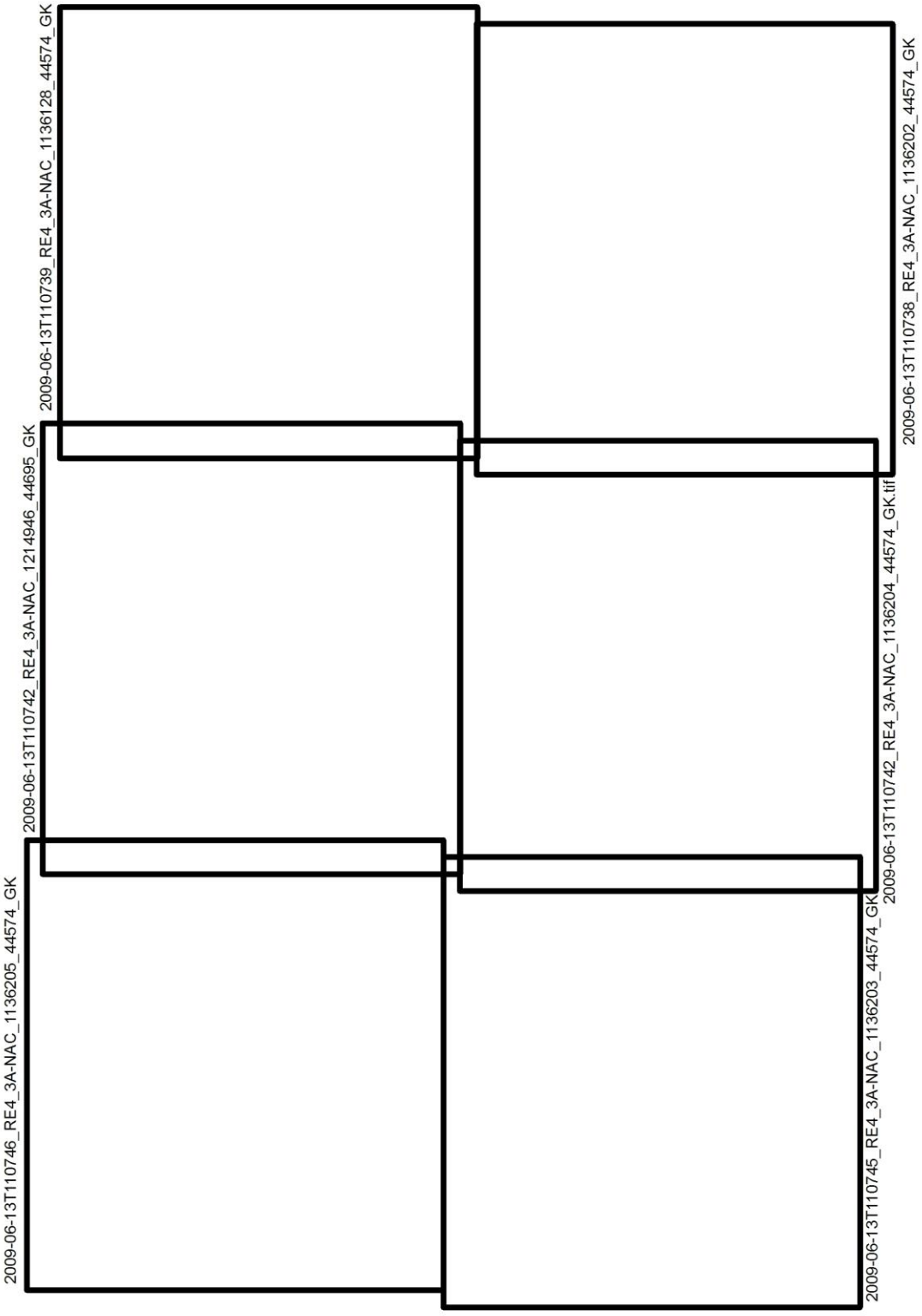


**Figure 2: Six RapidEye tiles acquired over the MFRA study area situated in central Germany.**

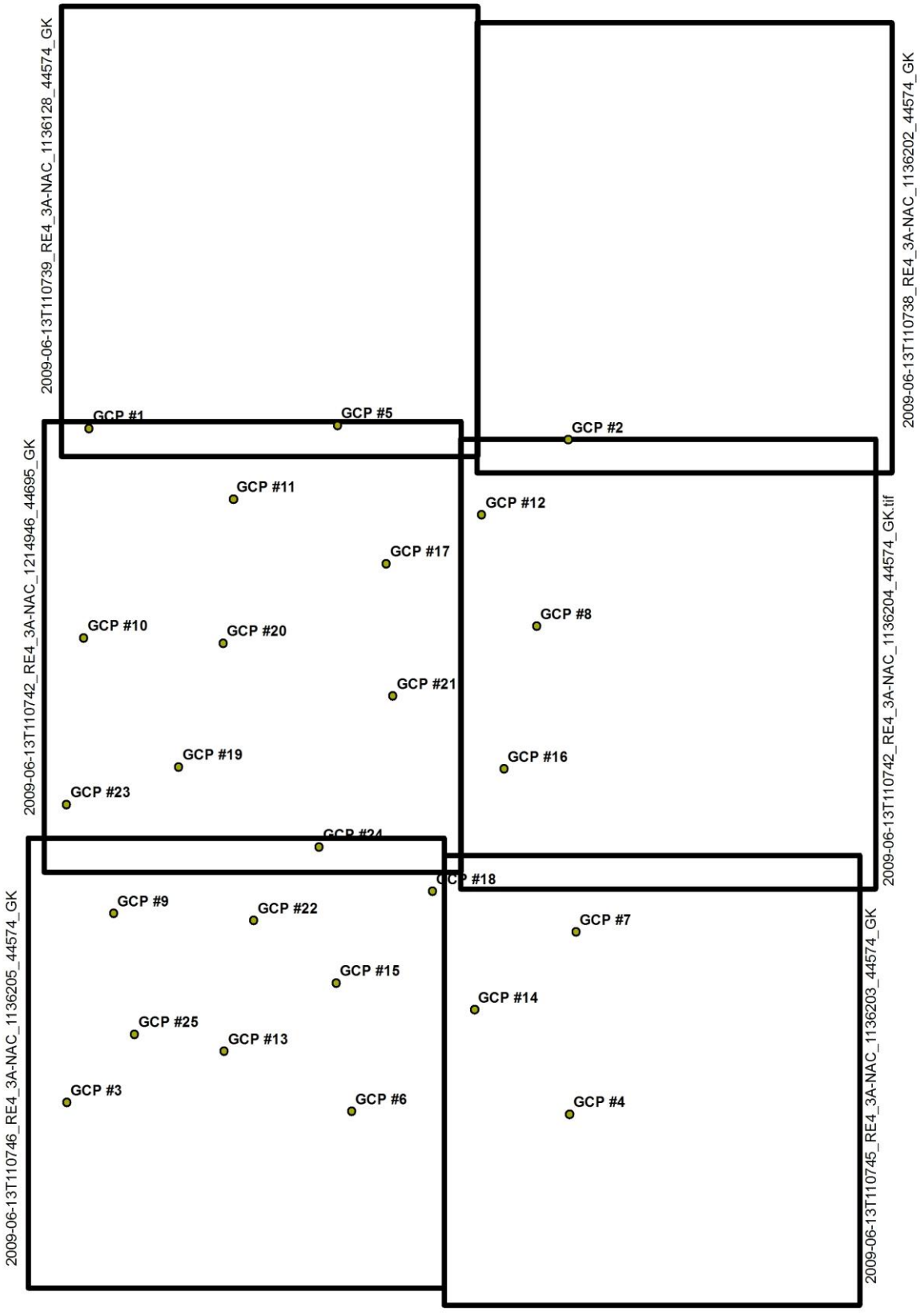


**Figure 3: Distribution of the 25 check points within the MFRA test zone.**

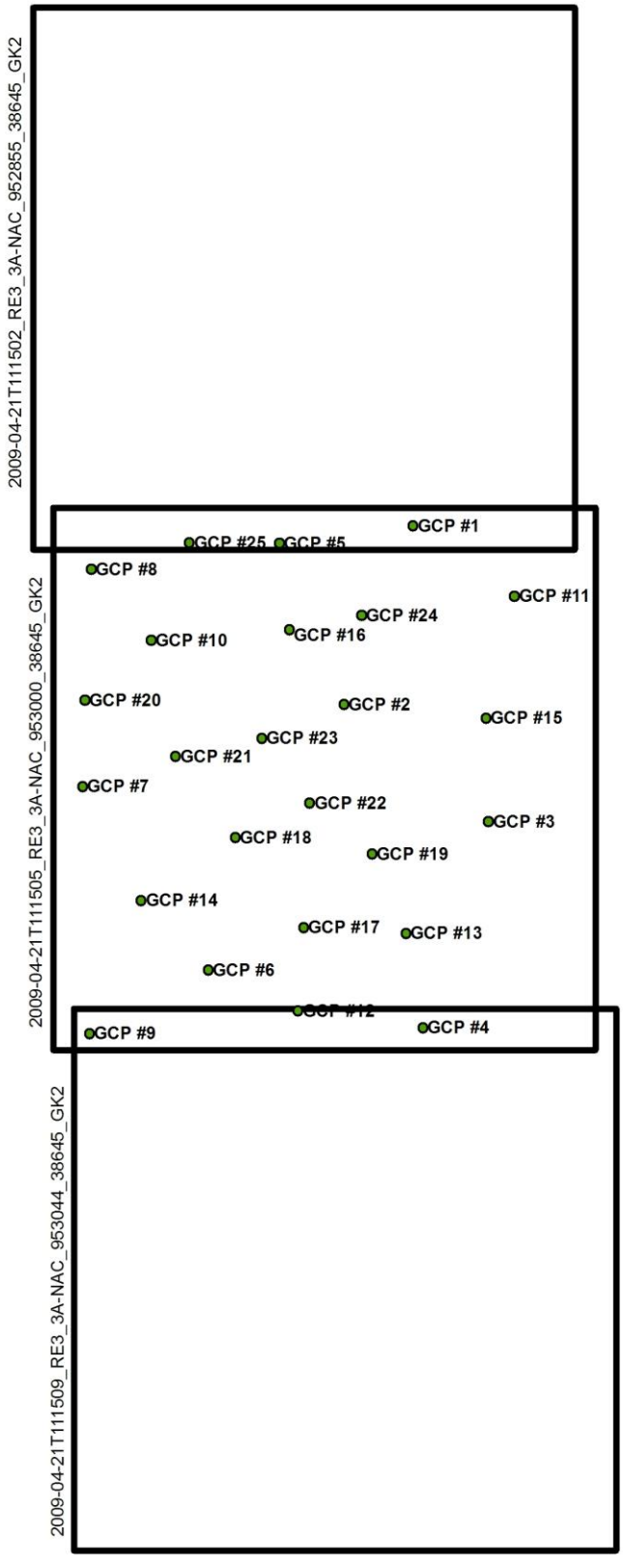


**Figure 4: Distribution of the 25 check points within the WEIL test zone.**

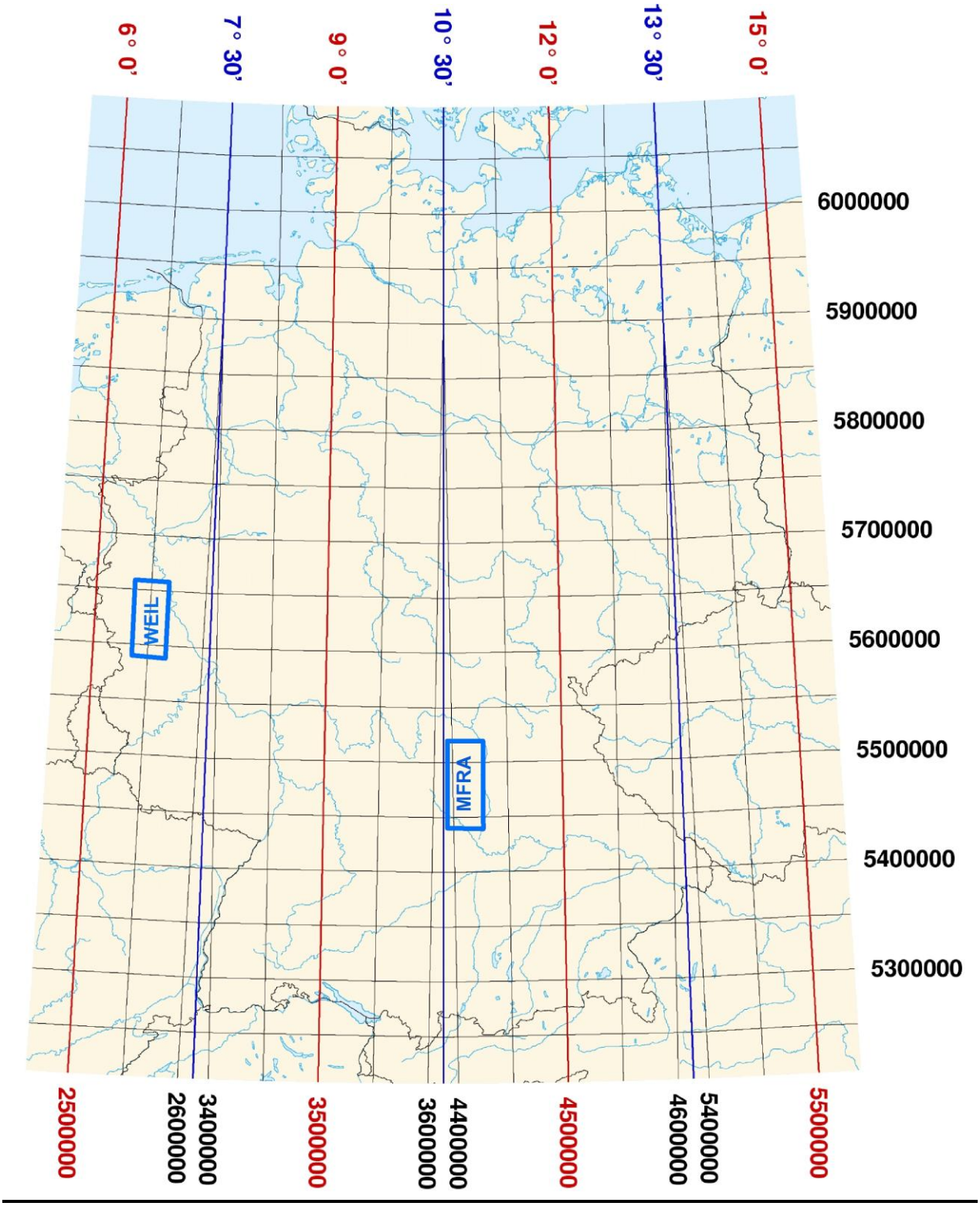


**Figure 5: WEIL and MFRA study areas displayed in Gauss-Krueger coordinate system (the central meridians are marked in red).**

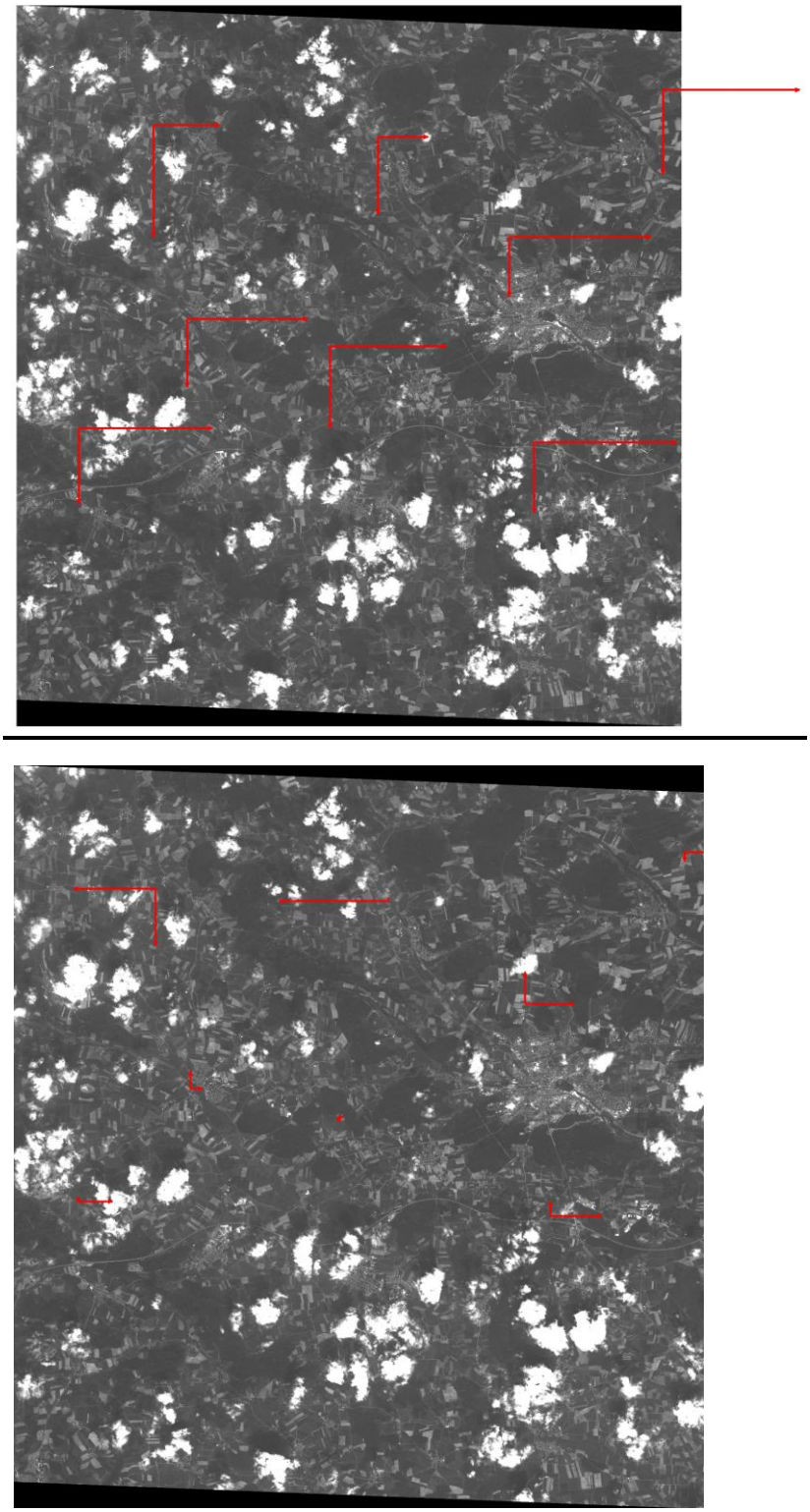

**Figure 6: MFRA2 - Differences (residuals) between the reference and measured check points coordinates prior and after shift-correction displayed with scale factor 500.**

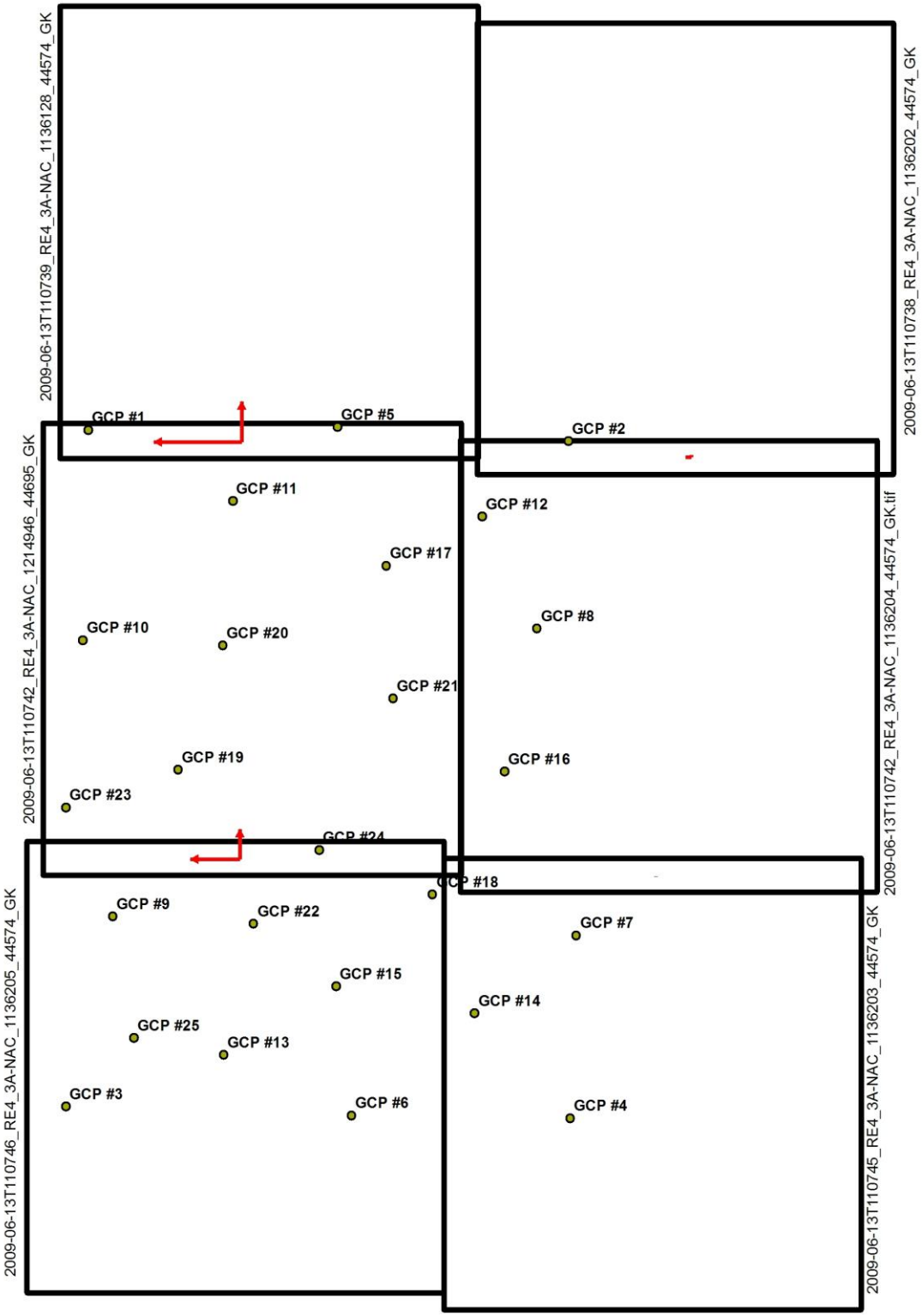


**Figure 7: Average shift in pixel locations between the overlying in South-North direction MFRA tile pairs.**

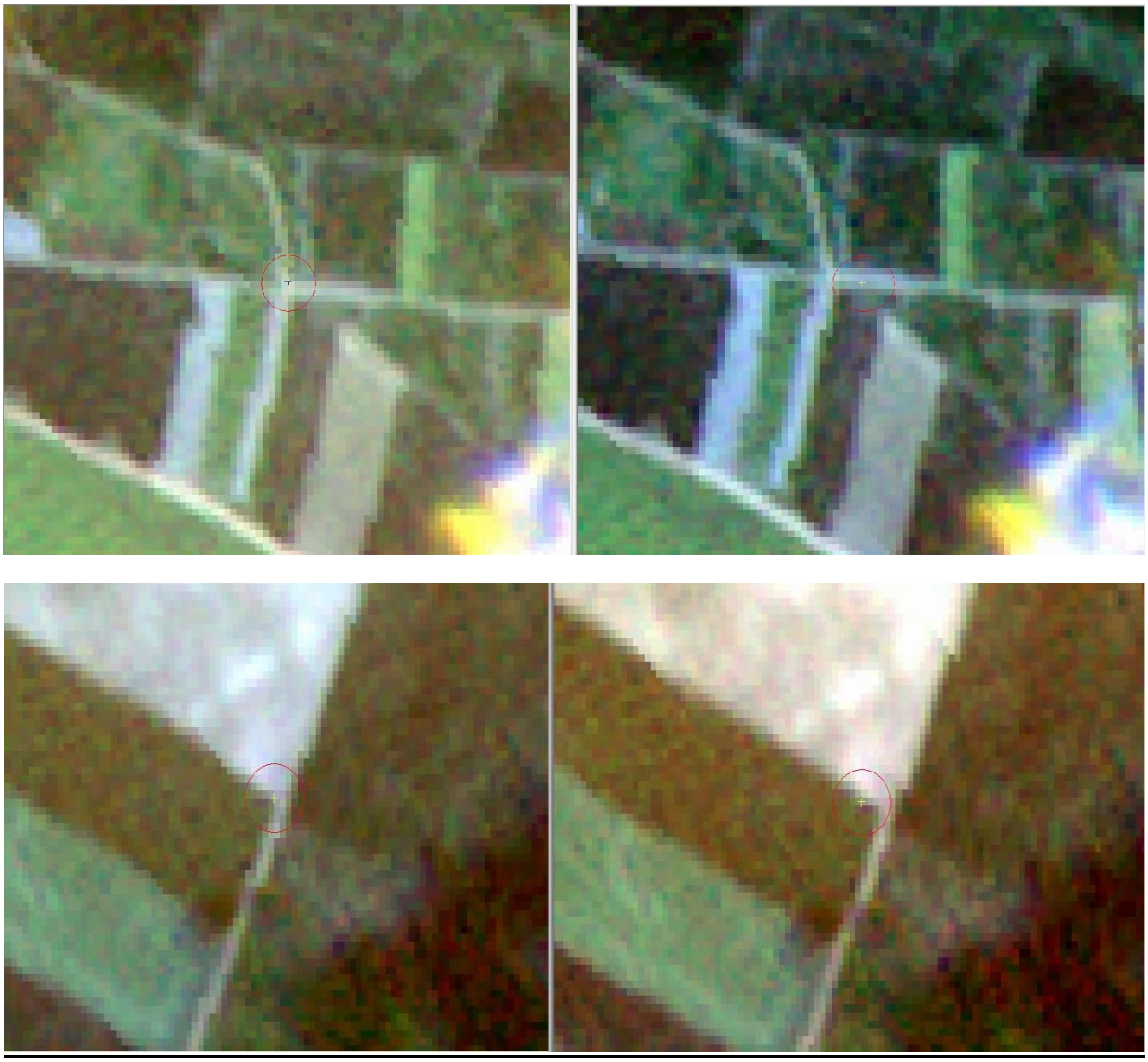

**Figure 8: Example of shift in pixel locations between the overlying in South-North direction tile pairs MFRA0/MFRA1 (CP#220; upper) and MFRA1/MFRA2 (CP#219; lower) projected in Gauss-Krueger.**

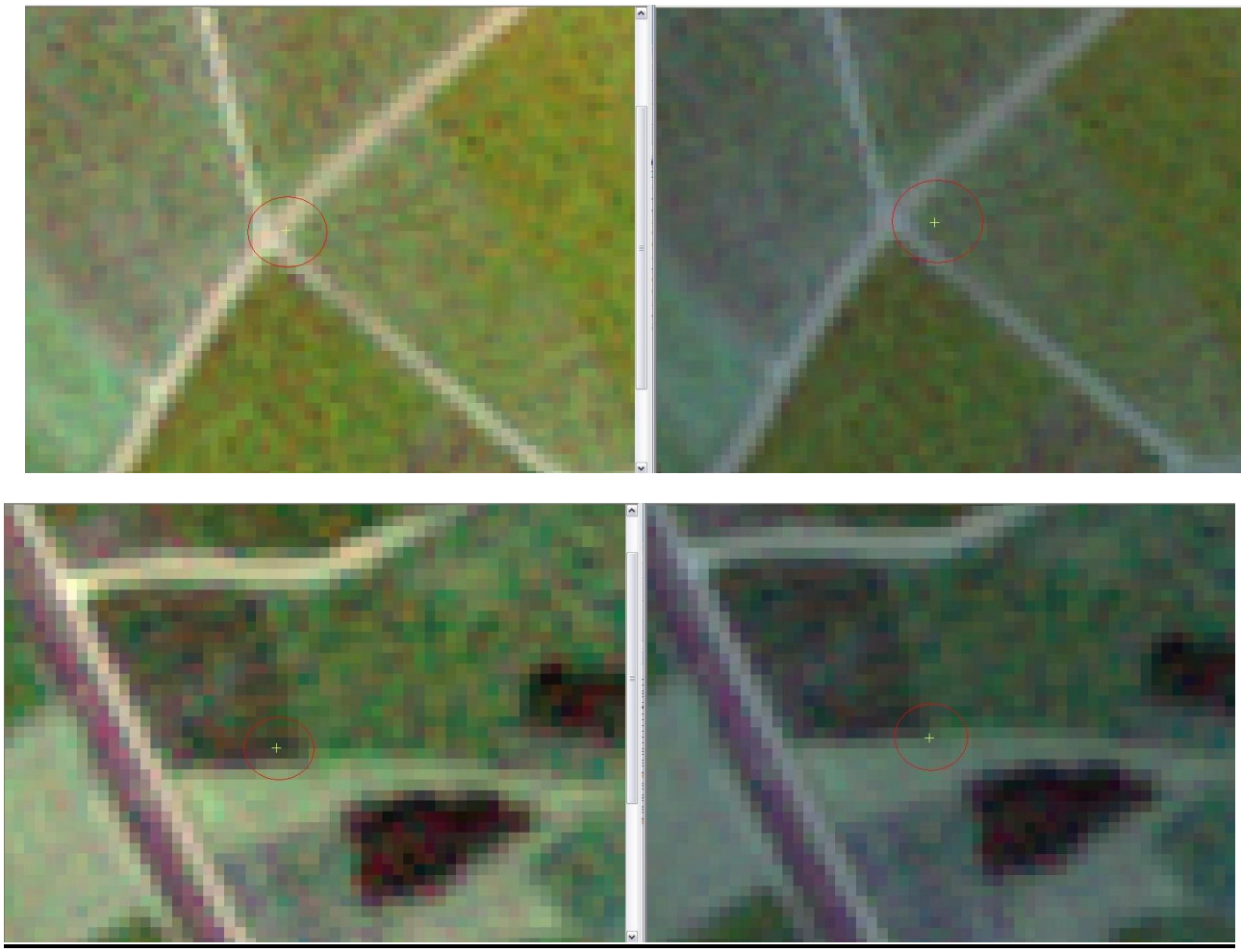

**Figure 9: Shift between the MFRA0/ MFRA1 (upper; CP#231) and MFRA1/MFRA2 tiles (lower; CP#242). Images projected in UTM.**

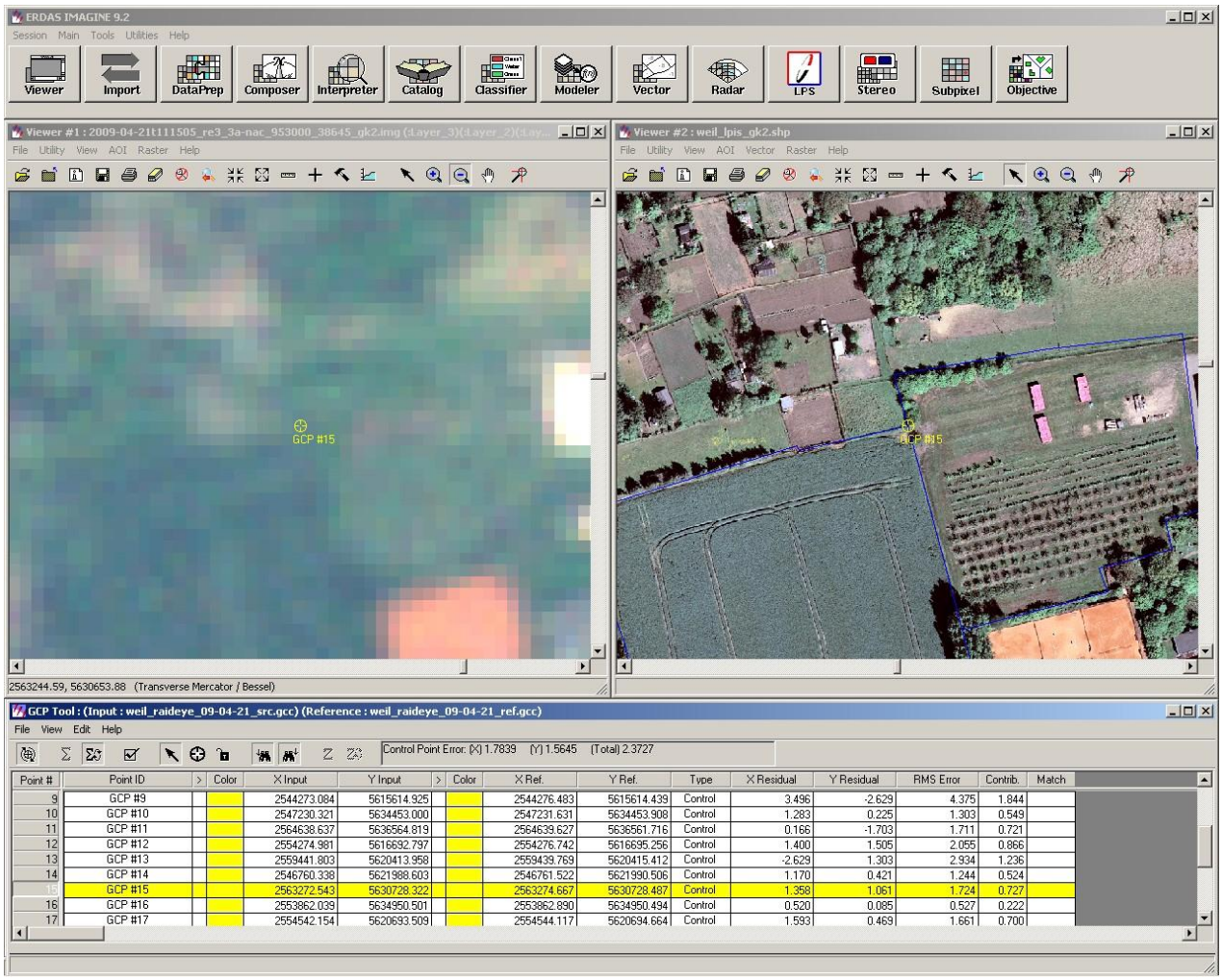


**Figure 10: Example of the wrongly-defined check point (WEIL GCP#15; EFTAS imagette).**

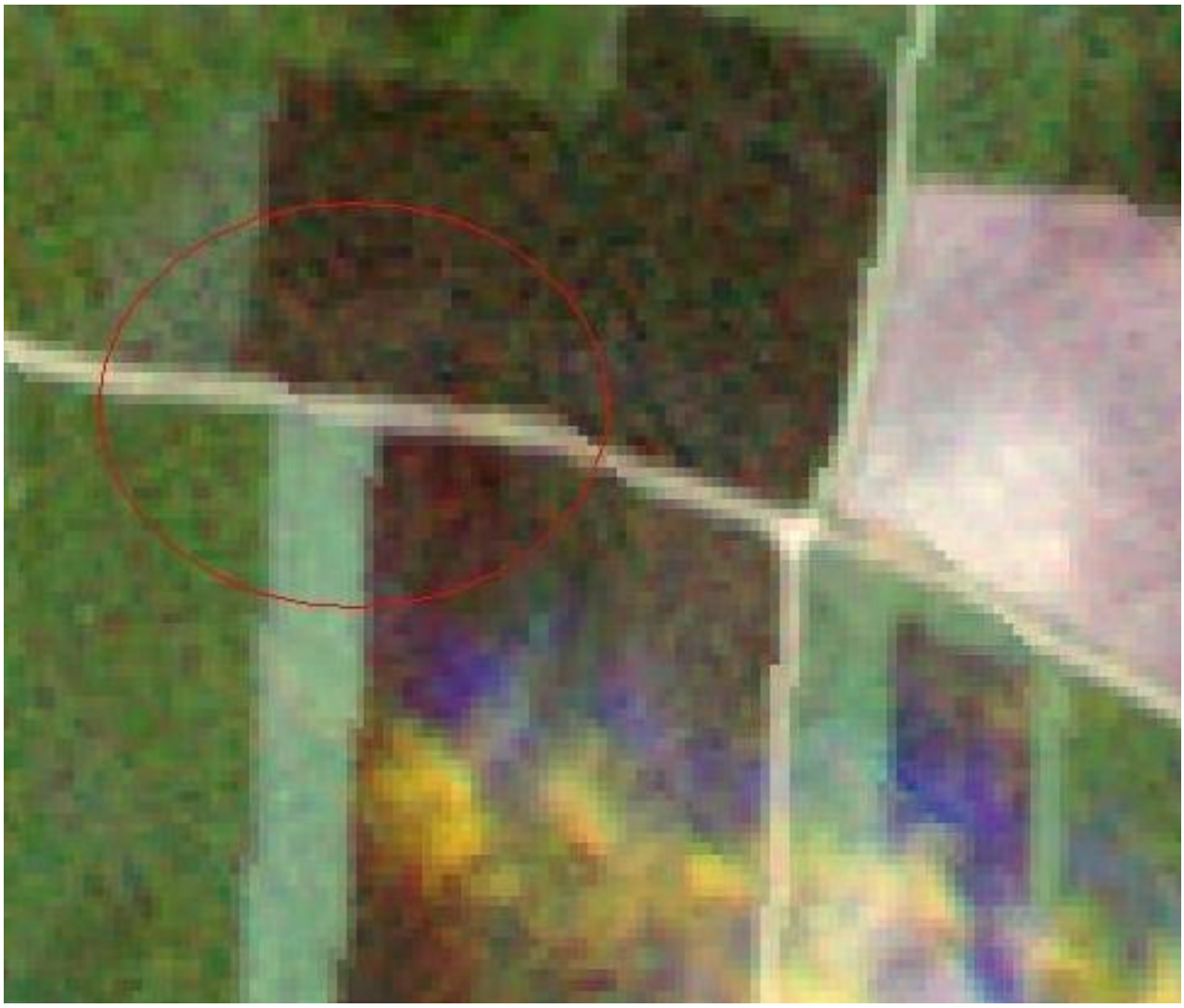

**Figure 11: The anomaly observed in close surroundings of GCP#3 on the MFRA ortho tiles reprojected to Gauss-Krueger by RapidEye using PCI Geomatica standard reprojection tools.**

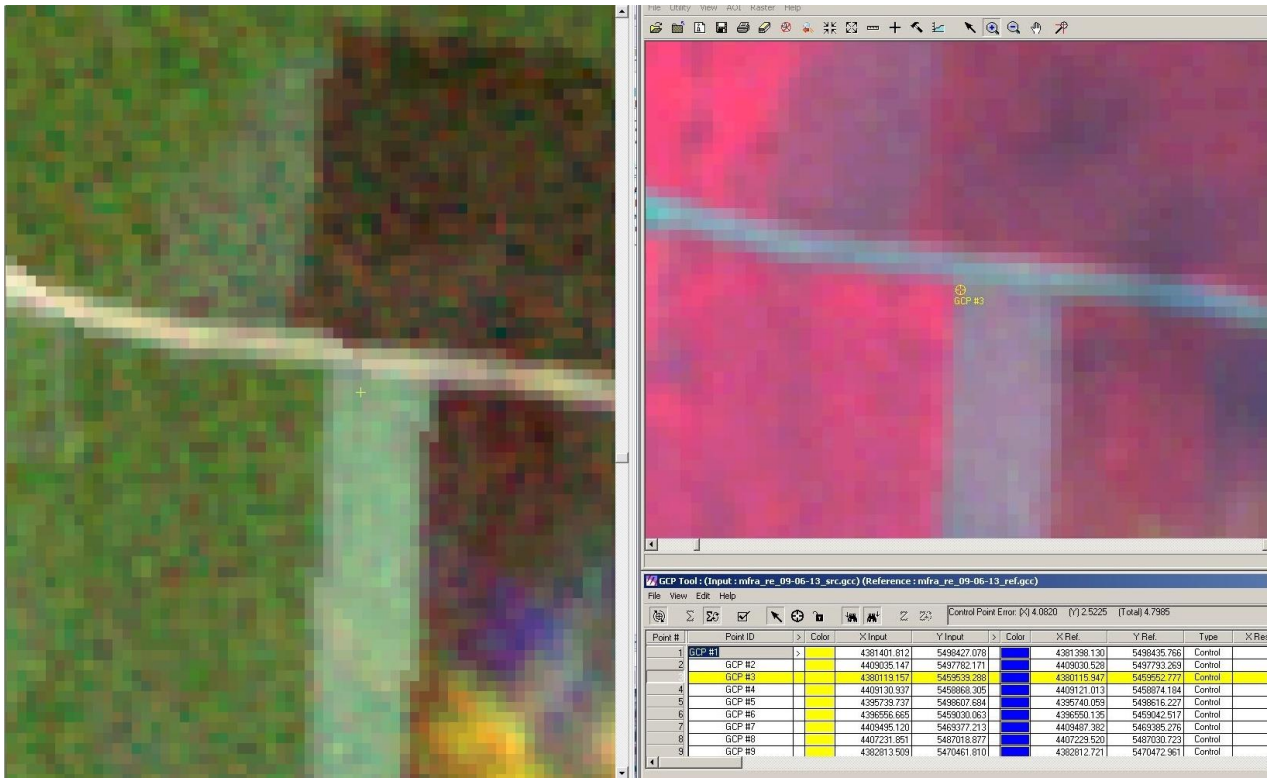


**Figure 12: The anomaly observed in close surroundings of GCP#3 on the MFRA ortho tiles reprojected to Gauss-Krueger by RapidEye using PCI Geomatica standard reprojection tools (left) and anomaly-free orthotile reprojected by EFTAS using ERDAS Imagine tools (right).**

## 12. Appendixes

Appendix 1: MFRA: Point identification error on RapidEye image product

Appendix 2: WEIL1: Point identification error on RapidEye image product

Appendix 3: External Quality Control (EQC) of MFRA site performed by EFTAS

Appendix 4: External Quality Control (EQC) of WEIL1 site performed by EFTAS

Appendix 5: Results of the external quality control MFRA site performed by the JRC

Appendix 6: Results of the external quality control of WEIL site performed by the JRC

Appendix 7.1: MFRA: Point identification error on LPIS data source

Appendix 7.2: WEIL1: Point identification error on LPIS data source

Appendix 8: Metadata summary and quality control results for the three tested LPIS-based RapidEye level 3A tiles (WEIL1, MFRA1, MFRA2)

Appendix 9.1: Shift measurements between MFRA1 and MFRA2 tiles projected in UTM (upper table) and Gauss-Krueger projection (lower table).

Appendix 9.2: Shift measurements between MFRA0 and MFRA1 tiles projected in UTM (upper table) and Gauss-Krueger projection (lower table).

| Iteration | GCP#2 | | GCP#22 | | GCP#7 | |
|---|---|---|---|---|---|---|
| | X (E) Measured [m] | Y (N) Measured [m] | X (E) Measured [m] | Y (N) Measured [m] | X (E) Measured [m] | Y (N) Measured [m] |
| 1 | 4409062.518 | 5497775.507 | 4390928.396 | 5470046.327 | 4409509.385 | 5469367.376 |
| 2 | 4409066.124 | 5497775.262 | 4390933.379 | 5470040.513 | 4409512.548 | 5469370.638 |
| 3 | 4409064.454 | 5497775.622 | 4390928.273 | 5470041.280 | 4409507.761 | 5469366.593 |
| 4 | 4409064.147 | 5497776.387 | 4390927.208 | 5470035.792 | 4409508.454 | 5469370.085 |
| 5 | 4409063.318 | 5497772.281 | 4390928.442 | 5470037.604 | 4409513.734 | 5469371.593 |
| 6 | 4409063.728 | 5497776.917 | 4390932.841 | 5470041.222 | 4409510.738 | 5469373.544 |
| 7 | 4409060.996 | 5497777.961 | 4390930.048 | 5470042.246 | 4409512.055 | 5469369.913 |
| 8 | 4409064.185 | 5497776.300 | 4390932.478 | 5470043.461 | 4409511.152 | 5469371.737 |
| 9 | 4409066.340 | 5497775.222 | 4390929.146 | 5470043.291 | 4409511.488 | 5469372.449 |
| 10 | 4409066.152 | 5497776.215 | 4390930.705 | 5470041.140 | 4409510.335 | 5469370.315 |
| Mean | 4409064.196 | 5497775.767 | 4390930.092 | 5470041.288 | 4409510.765 | 5469370.424 |
| Standard deviation | **1.71** | **1.48** | **2.17** | **2.97** | **1.85** | **2.14** |

**Appendix 1: MFRA: Point identification error on RapidEye image product**

| Iteration | GCP#2 | | GCP#15 | | GCP#12 | |
|---|---|---|---|---|---|---|
| | X (E) Measured [m] | Y (N) Measured [m] | X (E) Measured [m] | Y (N) Measured [m] | X (E) Measured [m] | Y (N) Measured [m] |
| 1 | 2556467.252 | 5631376.847 | 2563276.521 | 5630723.065 | 2554274.793 | 5616693.172 |
| 2 | 2556467.161 | 5631377.056 | 2563266.848 | 5630726.717 | 2554272.194 | 5616693.261 |
| 3 | 2556459.773 | 5631383.914 | 2563264.676 | 5630724.610 | 2554271.627 | 5616697.801 |
| 4 | 2556463.763 | 5631381.000 | 2563272.087 | 5630734.091 | 2554276.973 | 5616693.575 |
| 5 | 2556467.562 | 5631380.327 | 2563272.295 | 5630726.170 | 2554276.629 | 5616694.638 |
| 6 | 2556463.963 | 5631381.502 | 2563281.632 | 5630724.892 | 2554275.599 | 5616694.964 |
| 7 | 2556464.076 | 5631380.634 | 2563276.358 | 5630723.453 | 2554277.302 | 5616693.261 |
| 8 | 2556463.022 | 5631382.824 | 2563277.005 | 5630726.000 | 2554271.746 | 5616694.306 |
| 9 | 2556467.084 | 5631380.925 | 2563277.288 | 5630723.843 | 2554273.837 | 5616691.170 |
| 10 | 2556464.746 | 5631380.925 | 2563280.256 | 5630721.257 | 2554274.785 | 5616693.343 |
| Mean | 2556464.840 | 5631380.595 | 2563274.497 | 5630725.410 | 2554274.549 | 5616693.949 |
| Standard deviation | **2.48** | **2.21** | **5.49** | **3.46** | **2.15** | **1.71** |

**Appendix 2: WEIL1: Point identification error on RapidEye image product**

| GCP-ID | X-Satellitenbild | Y-Satellitenbild | X-Referenz | Y-Referenz | Δ X-Sat X-Referenz | Δ Y-Sat Y-Referenz | ΔX² | ΔY² |
|---|---|---|---|---|---|---|---|---|
| GCP #1 | 4381401.8118 | 5498427.0776 | 4381398.1298 | 5498435.7662 | 3.6820 | -8.6886 | 13.5569 | 75.4910 |
| GCP #2 | 4409035.1466 | 5497782.1711 | 4409030.5280 | 5497793.2690 | 4.6186 | -11.0979 | 21.3314 | 123.1641 |
| GCP #3 | 4380119.1566 | 5459539.2878 | 4380115.9473 | 5459552.7766 | 3.2093 | -13.4888 | 10.2997 | 181.9475 |
| GCP #4 | 4409130.9368 | 5458868.3045 | 4409121.0125 | 5458874.1839 | 9.9243 | -5.8794 | 98.4921 | 34.5673 |
| GCP #5 | 4395739.7375 | 5498607.6838 | 4395740.0589 | 5498616.2269 | -0.3215 | -8.5431 | 0.1033 | 72.9840 |
| GCP #6 | 4396556.6652 | 5459030.0635 | 4396550.1349 | 5459042.5166 | 6.5304 | -12.4531 | 42.6456 | 155.0797 |
| GCP #7 | 4409495.1203 | 5469377.2128 | 4409487.3824 | 5469385.2761 | 7.7380 | -8.0633 | 59.8761 | 65.0164 |
| GCP #8 | 4407231.8509 | 5487018.8766 | 4407229.5197 | 5487030.7229 | 2.3312 | -11.8463 | 5.4343 | 140.3355 |
| GCP #9 | 4382813.5092 | 5470461.8103 | 4382812.7207 | 5470472.9612 | 0.7884 | -11.1510 | 0.6216 | 124.3440 |
| GCP #10 | 4381087.4114 | 5486349.4733 | 4381084.8509 | 5486356.1106 | 2.5604 | -6.6372 | 6.5559 | 44.0526 |
| GCP #11 | 4389722.5764 | 5494352.7011 | 4389716.6917 | 5494355.3616 | 5.8847 | -2.6605 | 34.6297 | 7.0784 |
| GCP #12 | 4404060.6550 | 5493451.9875 | 4404055.1718 | 5493460.2788 | 5.4832 | -8.2913 | 30.0651 | 68.7458 |
| GCP #13 | 4389193.9229 | 5462501.1028 | 4389188.2187 | 5462506.7543 | 5.7042 | -5.6514 | 32.5378 | 31.9388 |
| GCP #14 | 4403632.4888 | 5464892.2432 | 4403628.3387 | 5464898.7354 | 4.1501 | -6.4923 | 17.2230 | 42.1493 |
| GCP #15 | 4395660.4631 | 5466440.0815 | 4395661.0595 | 5466449.3683 | -0.5964 | -9.2868 | 0.3557 | 86.2446 |
| GCP #16 | 4405349.4830 | 5478788.6003 | 4405341.5190 | 5478796.2792 | 7.9640 | -7.6789 | 63.4255 | 58.9648 |
| GCP #17 | 4398547.0765 | 5490624.0771 | 4398549.4678 | 5490630.0609 | -2.3913 | -5.9838 | 5.7183 | 35.8059 |
| GCP #18 | 4401219.2082 | 5471735.3688 | 4401216.8360 | 5471742.9270 | 2.3722 | -7.5582 | 5.6275 | 57.1266 |
| GCP #19 | 4386571.6383 | 5478900.3850 | 4386578.0997 | 5478908.9378 | -6.4614 | -8.5528 | 41.7498 | 73.1509 |
| GCP #20 | 4389138.3465 | 5486043.8046 | 4389144.7108 | 5486049.5994 | -6.3643 | -5.7949 | 40.5045 | 33.5804 |
| GCP #21 | 4398936.9614 | 5482999.3027 | 4398928.4737 | 5483009.1745 | 8.4877 | -9.8718 | 72.0408 | 97.4516 |
| GCP #22 | 4390912.8475 | 5470044.1149 | 4390920.9242 | 5470050.0659 | -8.0767 | -5.9510 | 65.2332 | 35.4142 |
| GCP #23 | 4380103.7941 | 5476734.0812 | 4380104.3207 | 5476738.2906 | -0.5267 | -4.2094 | 0.2774 | 17.7194 |
| GCP #24 | 4394681.5268 | 5474292.3347 | 4394680.9617 | 5474301.6969 | 0.5651 | -9.3622 | 0.3193 | 87.6503 |
| GCP #25 | 4384025.7703 | 5463480.6932 | 4384025.6911 | 5463490.2707 | 0.0792 | -9.5775 | 0.0063 | 91.7285 |
| | | | | | | **Σ** | 668.6310 | 1841.7318 |

| | |
|---|---|
| **RMS X** | 5.171579912 |
| **RMS Y** | 8.583080485 |

| | |
|---|---|
| **Σ (ΔX²ΔY²)** | 2510.362735 |
| **{Σ (ΔX²ΔY²)} / (ΣGCP's-1)** | 104.5984473 |
| **Genauigkeit [m]** | 10.22733823 |

| GCP-ID | X-Satellitenbild | Y-Satellitenbild | X-Referenz | Y-Referenz | Δ X-Sat X-Referenz | Δ Y-Sat Y-Referenz | ΔX² | ΔY² |
|---|---|---|---|---|---|---|---|---|
| GCP #1 | 2559787.2913 | 5639940.1425 | 2559790.9554 | 5639937.6952 | -3.6641 | 2.4474 | 13.4256 | 5.9896 |
| GCP #2 | 2556469.1538 | 5631379.6691 | 2556467.8777 | 5631383.1250 | 1.2761 | -3.4558 | 1.6285 | 11.9427 |
| GCP #3 | 2563389.5103 | 5625758.9597 | 2563388.2503 | 5625756.8380 | 1.2600 | 2.1217 | 1.5877 | 4.5014 |
| GCP #4 | 2560260.0111 | 5615891.9170 | 2560261.5858 | 5615892.6063 | -1.5747 | -0.6893 | 2.4797 | 0.4752 |
| GCP #5 | 2553368.8585 | 5639091.6975 | 2553366.8300 | 5639090.0713 | 2.0285 | 1.6262 | 4.1148 | 2.6445 |
| GCP #6 | 2549966.1933 | 5618657.1944 | 2549963.4684 | 5618659.7525 | 2.7249 | -2.5581 | 7.4249 | 6.5440 |
| GCP #7 | 2543955.7602 | 5627452.3851 | 2543954.5223 | 5627452.6892 | 1.2379 | -0.3042 | 1.5323 | 0.0925 |
| GCP #8 | 2544358.4645 | 5637850.4672 | 2544359.3189 | 5637853.1928 | -0.8544 | -2.7256 | 0.7300 | 7.4289 |
| GCP #9 | 2544273.0836 | 5615614.9251 | 2544276.4827 | 5615614.4394 | -3.3991 | 0.4857 | 11.5535 | 0.2359 |
| GCP #10 | 2547230.3209 | 5634453.0003 | 2547231.6314 | 5634453.9077 | -1.3105 | -0.9073 | 1.7173 | 0.8232 |
| GCP #11 | 2564638.6371 | 5636564.8192 | 2564639.6265 | 5636561.7160 | -0.9895 | 3.1032 | 0.9791 | 9.6298 |
| GCP #12 | 2554274.9813 | 5616692.7966 | 2554276.7417 | 5616695.2562 | -1.7604 | -2.4596 | 3.0990 | 6.0495 |
| GCP #13 | 2559441.8026 | 5620413.9575 | 2559439.7688 | 5620415.4124 | 2.0338 | -1.4549 | 4.1362 | 2.1167 |
| GCP #14 | 2546760.3382 | 5621988.6028 | 2546761.5215 | 5621990.5059 | -1.1833 | -1.9032 | 1.4001 | 3.6221 |
| GCP #15 | 2563272.5435 | 5630728.3225 | 2563274.6665 | 5630728.4868 | -2.1230 | -0.1643 | 4.5073 | 0.0270 |
| GCP #16 | 2553862.0392 | 5634950.5009 | 2553862.8901 | 5634950.4936 | -0.8509 | 0.0073 | 0.7240 | 0.0001 |
| GCP #17 | 2554542.1540 | 5620693.5093 | 2554544.1173 | 5620694.6639 | -1.9633 | -1.1546 | 3.8544 | 1.3331 |
| GCP #18 | 2551258.4584 | 5624998.8312 | 2551257.8958 | 5624998.8765 | 0.5626 | -0.0453 | 0.3165 | 0.0021 |
| GCP #19 | 2557809.5129 | 5624205.9945 | 2557808.7627 | 5624204.4941 | 0.7503 | 1.5004 | 0.5629 | 2.2511 |
| GCP #20 | 2544057.9041 | 5631581.1439 | 2544055.8302 | 5631579.7368 | 2.0739 | 1.4071 | 4.3012 | 1.9800 |
| GCP #21 | 2548406.6717 | 5628891.2787 | 2548406.4152 | 5628893.3174 | 0.2566 | -2.0387 | 0.0658 | 4.1561 |
| GCP #22 | 2554832.7791 | 5626651.3431 | 2554834.2546 | 5626651.9677 | -1.4754 | -0.6246 | 2.1769 | 0.3901 |
| GCP #23 | 2552540.1297 | 5629762.5632 | 2552538.6978 | 5629762.0162 | 1.4318 | 0.5470 | 2.0501 | 0.2992 |
| GCP #24 | 2557306.3671 | 5635646.4501 | 2557309.4023 | 5635645.1928 | -3.0352 | 1.2572 | 9.2123 | 1.5807 |
| GCP #25 | 2549067.1584 | 5639127.1183 | 2549066.4539 | 5639129.9821 | 0.7045 | -2.8638 | 0.4964 | 8.2016 |
| | | | | | | Σ | 84.0765 | 82.3171 |

| | |
|---|---|
| RMS X | 1.833864649 |
| RMS Y | 1.814574919 |

| | |
|---|---|
| Σ (ΔX²ΔY²) | 166.3935422 |
| {Σ (ΔX²ΔY²)} / (ΣGCP's-1) | 6.933064258 |
| Genauigkeit [m] | 2.633071259 |

| ID | X (E) Reference [m] | Y (N) Reference [m] | X (E) Measured [m] | Y (N) Measured [m] | X (E) Difference [m] | Y (N) Difference [m] | X (E) Difference ^ 2 | Y (N) Difference ^ 2 | Image ID |
|---|---|---|---|---|---|---|---|---|---|
| GCP #1 | 4381398.1298 | 5498435.7662 | 4381428.237 | 5498424.664 | 30.1072 | -11.1022 | 906.4413343 | 123.2579826 | 1136128_44574_GK |
| GCP #2 | 4409030.5280 | 5497793.2690 | 4409066.141 | 5497775.234 | 35.6130 | -18.0350 | 1268.283349 | 325.2623832 | 1136202_44574_GK |
| GCP #3 | 4380115.9473 | 5459552.7766 | 4380132.045 | 5459543.641 | 16.0977 | -9.1356 | 259.1349224 | 83.45887146 | 1136205_44574_GK |
| GCP #4 | 4409121.0125 | 5458874.1839 | 4409152.561 | 5458861.811 | 31.5485 | -12.3729 | 995.3071228 | 153.0891733 | 1136203_44574_GK |
| GCP #5 | 4395740.0589 | 5498616.2269 | 4395764.147 | 5498609.160 | 24.0881 | -7.0669 | 580.236009 | 49.94128267 | 1136128_44574_GK |
| GCP #6 | 4396550.1349 | 5459042.5166 | 4396567.359 | 5459034.051 | 17.2241 | -8.4656 | 296.6706088 | 71.66558065 | 1136205_44574_GK |
| GCP #7 | 4409487.3824 | 5469385.2761 | 4409514.165 | 5469368.707 | 26.7826 | -16.5691 | 717.3089821 | 274.534821 | 1136203_44574_GK |
| GCP #8 | 4407229.5197 | 5487030.7229 | 4407253.904 | 5487014.284 | 24.3843 | -16.4389 | 594.5943411 | 270.2371084 | 1136204_44574_GK |
| GCP #9 | 4382812.7207 | 5470472.9612 | 4382820.693 | 5470459.502 | 7.9723 | -13.4592 | 63.55684261 | 181.1506789 | 1136205_44574_GK |
| GCP #10 | 4381084.8509 | 5486356.1106 | 4381085.065 | 5486353.125 | 0.2141 | -2.9856 | 0.045820558 | 8.913539613 | 1214946_44695_GK |
| GCP #11 | 4389716.6917 | 5494355.3616 | 4389720.644 | 5494355.327 | 3.9523 | -0.0346 | 15.62063395 | 0.001196453 | 1214946_44695_GK |
| GCP #12 | 4404055.1718 | 5493460.2788 | 4404077.714 | 5493446.963 | 22.5422 | -13.3158 | 508.149711 | 177.3095629 | 1136204_44574_GK |
| GCP #13 | 4389188.2187 | 5462506.7543 | 4389202.206 | 5462496.911 | 13.9873 | -9.8433 | 195.6436932 | 96.88974065 | 1136205_44574_GK |
| GCP #14 | 4403628.3387 | 5464898.7354 | 4403649.286 | 5464886.167 | 20.9473 | -12.5684 | 438.7887501 | 157.9655691 | 1136203_44574_GK |
| GCP #15 | 4395661.0595 | 5466449.3683 | 4395678.178 | 5466442.160 | 17.1185 | -7.2083 | 293.0446052 | 51.95947268 | 1136205_44574_GK |
| GCP #16 | 4405341.5190 | 5478796.2792 | 4405367.590 | 5478782.099 | 26.0710 | -14.1802 | 679.6984874 | 201.0777124 | 1136204_44574_GK |
| GCP #17 | 4398549.4678 | 5490630.0609 | 4398548.129 | 5490635.209 | -1.3388 | 5.1481 | 1.792471232 | 26.50269906 | 1214946_44695_GK |
| GCP #18 | 4401216.8360 | 5471742.9270 | 4401233.295 | 5471732.815 | 16.4590 | -10.1120 | 270.8994322 | 102.2532953 | 1136205_44574_GK |
| GCP #19 | 4386578.0997 | 5478908.9378 | 4386570.111 | 5478905.673 | -7.9887 | -3.2648 | 63.81937914 | 10.65910565 | 1214946_44695_GK |
| GCP #20 | 4389144.7108 | 5486049.5994 | 4389136.310 | 5486049.449 | -8.4008 | -0.1504 | 70.57422965 | 0.022633409 | 1214946_44695_GK |
| GCP #21 | 4398928.4737 | 5483009.1745 | 4398935.742 | 5483008.578 | 7.2683 | -0.5965 | 52.82762814 | 0.355793604 | 1214946_44695_GK |
| GCP #22 | 4390920.9242 | 5470050.0659 | 4390926.976 | 5470040.772 | 6.0518 | -9.2939 | 36.6236927 | 86.37666328 | 1136205_44574_GK |
| GCP #23 | 4380104.3207 | 5476738.2906 | 4380105.528 | 5476735.973 | 1.2073 | -2.3176 | 1.457464586 | 5.371459202 | 1214946_44695_GK |
| GCP #24 | 4394680.9617 | 5474301.6969 | 4394683.283 | 5474304.068 | 2.3213 | 2.3711 | 5.388365677 | 5.62232785 | 1214946_44695_GK |
| GCP #25 | 4384025.6911 | 5463490.2707 | 4384040.229 | 5463482.052 | 14.5379 | -8.2187 | 211.3506016 | 67.54701308 | 1136205_44574_GK |
| | GCP #1 is available on two images | | | | | | | | |
| GCP#1 | 4381398.1298 | 5498435.7662 | 4381399.764 | 5498434.792 | 1.6342 | -0.9742 | | | 1214946_44695_GK |

| | |
|---|---|
| RMSE X (E) [m] (total 25 GCP) | **18.47** |
| RMSE Y (N) [m] (total 25 GCP) | **10.06** |
| RMSE X (E) [m] (MFRA1) | **5.14** |
| RMSE Y (N) [m] (MFRA1) | **2.68** |
| RMSE X (E) [m] (MFRA2) | **14.26** |
| RMSE Y (N) [m] (MFRA2) | **9.63** |

**Appendix 5: Results of the External Quality Control MFRA site performed by the JRC**

| ID | X (E) Reference [m] | Y (N) Reference [m] | X (E) Measured [m] | Y (N) Measured [m] | X (E) Difference [m] | Y (N) Difference [m] | X (E) Difference ^ 2 | Y (N) Difference ^ 2 | Image ID |
|---|---|---|---|---|---|---|---|---|---|
| GCP #1 | 2559787.2913 | 5639940.1425 | 2559783.485 | 5639938.434 | -3.8063 | -1.7085 | 14.48756144 | 2.919093281 | 953000_38645_GK2 |
| GCP #2 | 2556469.1538 | 5631379.6691 | 2556470.155 | 5631380.649 | 1.0012 | 0.9799 | 1.002357387 | 0.960149469 | 953000_38645_GK2 |
| GCP #3 | 2563389.5103 | 5625758.9597 | 2563388.907 | 5625759.787 | -0.6033 | 0.8273 | 0.363977683 | 0.684506632 | 953000_38645_GK2 |
| GCP #4 | 2560260.0111 | 5615891.9170 | 2560259.717 | 5615893.771 | -0.2941 | 1.8540 | 0.086513216 | 3.437474111 | 953000_38645_GK2 |
| GCP #5 | 2553368.8585 | 5639091.6975 | 2553369.894 | 5639091.097 | 1.0355 | -0.6005 | 1.072270853 | 0.360563452 | 953000_38645_GK2 |
| GCP #6 | 2549966.1933 | 5618657.1944 | 2549970.168 | 5618654.827 | 3.9747 | -2.3674 | 15.79848112 | 5.60461207 | 953000_38645_GK2 |
| GCP #7 | 2543955.7602 | 5627452.3851 | 2543956.434 | 5627454.818 | 0.6738 | 2.4329 | 0.454067892 | 5.919240202 | 953000_38645_GK2 |
| GCP #8 | 2544358.4645 | 5637850.4672 | 2544358.132 | 5637851.404 | -0.3325 | 0.9368 | 0.110541946 | 0.87758639 | 953000_38645_GK2 |
| GCP #9 | 2544273.0836 | 5615614.9251 | 2544271.064 | 5615612.075 | -2.0196 | -2.8501 | 4.078902267 | 8.123126725 | 953000_38645_GK2 |
| GCP #10 | 2547230.3209 | 5634453.0003 | 2547227.524 | 5634451.968 | -2.7969 | -1.0323 | 7.822678362 | 1.065740658 | 953000_38645_GK2 |
| GCP #11 | 2564638.6371 | 5636564.8192 | 2564637.249 | 5636566.335 | -1.3881 | 1.5158 | 1.926725916 | 2.297782517 | 953000_38645_GK2 |
| GCP #12 | 2554274.9813 | 5616692.7966 | 2554272.378 | 5616694.195 | -2.6033 | 1.3984 | 6.77698866 | 1.955409515 | 953000_38645_GK2 |
| GCP #13 | 2559441.8026 | 5620413.9575 | 2559442.046 | 5620416.477 | 0.2434 | 2.5195 | 0.059264446 | 6.34782825 | 953000_38645_GK2 |
| GCP #14 | 2546760.3382 | 5621988.6028 | 2546756.532 | 5621988.777 | -3.8062 | 0.1742 | 14.48745738 | 0.030353905 | 953000_38645_GK2 |
| GCP #15 | 2563272.5435 | 5630728.3225 | 2563269.309 | 5630724.370 | -3.2345 | -3.9525 | 10.46184444 | 15.62217562 | 953000_38645_GK2 |
| GCP #16 | 2553862.0392 | 5634950.5009 | 2553858.627 | 5634949.294 | -3.4122 | -1.2069 | 11.64324035 | 1.456500971 | 953000_38645_GK2 |
| GCP #17 | 2554542.1540 | 5620693.5093 | 2554542.627 | 5620693.810 | 0.4730 | 0.3007 | 0.223720353 | 0.090418048 | 953000_38645_GK2 |
| GCP #18 | 2551258.4584 | 5624998.8312 | 2551261.859 | 5625000.467 | 3.4006 | 1.6358 | 11.56391999 | 2.676001427 | 953000_38645_GK2 |
| GCP #19 | 2557809.5129 | 5624205.9945 | 2557814.395 | 5624205.423 | 4.8821 | -0.5715 | 23.83445624 | 0.326599231 | 953000_38645_GK2 |
| GCP #20 | 2544057.9041 | 5631581.1439 | 2544056.710 | 5631585.172 | -1.1941 | 4.0281 | 1.42598916 | 16.22542446 | 953000_38645_GK2 |
| GCP #21 | 2548406.6717 | 5628891.2787 | 2548411.989 | 5628894.740 | 5.3173 | 3.4613 | 28.27325114 | 11.98057194 | 953000_38645_GK2 |
| GCP #22 | 2554832.7791 | 5626651.3431 | 2554834.497 | 5626658.329 | 1.7179 | 6.9859 | 2.95102563 | 48.8022514 | 953000_38645_GK2 |
| GCP #23 | 2552540.1297 | 5629762.5632 | 2552541.752 | 5629762.395 | 1.6223 | -0.1682 | 2.631951351 | 0.028299055 | 953000_38645_GK2 |
| GCP #24 | 2557306.3671 | 5635646.4501 | 2557308.480 | 5635650.519 | 2.1129 | 4.0689 | 4.464295151 | 16.55622154 | 953000_38645_GK2 |
| GCP #25 | 2549067.1584 | 5639127.1183 | 2549067.623 | 5639121.401 | 0.4646 | -5.7173 | 0.215821438 | 32.68700417 | 953000_38645_GK2 |

| | |
|---|---|
| RMSE X (E) [m] | **2.58** |
| RMSE Y (N) [m] | **2.74** |

**Appendix 6: Results of the External Quality Control of WEIL1 site performed by the JRC**

| GCP-ID | X-Satellitenbild | Y-Satellitenbild | X-Referenz | Y-Referenz | Δ X-Sat X-Referenz | Δ Y-Sat Y-Referenz | ΔX² | ΔY² |
|---|---|---|---|---|---|---|---|---|
| GCP #1 | 4381398.1298 | 5498435.7662 | 4381398.1305 | 5498435.7704 | -0.0007 | -0.0042 | 0.0000 | 0.0000 |
| GCP #2 | 4409030.5280 | 5497793.2690 | 4409030.5293 | 5497793.2628 | -0.0012 | 0.0063 | 0.0000 | 0.0000 |
| GCP #3 | 4380115.9473 | 5459552.7766 | 4380115.9120 | 5459552.7954 | 0.0353 | -0.0188 | 0.0012 | 0.0004 |
| GCP #4 | 4409121.0125 | 5458874.1839 | 4409121.0401 | 5458874.2505 | -0.0276 | -0.0666 | 0.0008 | 0.0044 |
| GCP #5 | 4395740.0589 | 5498616.2269 | 4395740.0600 | 5498616.2299 | -0.0011 | -0.0030 | 0.0000 | 0.0000 |
| GCP #6 | 4396550.1349 | 5459042.5166 | 4396550.1300 | 5459042.5099 | 0.0048 | 0.0067 | 0.0000 | 0.0000 |
| GCP #7 | 4409487.3824 | 5469385.2761 | 4409487.3778 | 5469385.2795 | 0.0046 | -0.0034 | 0.0000 | 0.0000 |
| GCP #8 | 4407229.5197 | 5487030.7229 | 4407229.5198 | 5487030.7198 | -0.0001 | 0.0031 | 0.0000 | 0.0000 |
| GCP #9 | 4382812.7207 | 5470472.9612 | 4382812.7200 | 5470472.9599 | 0.0007 | 0.0014 | 0.0000 | 0.0000 |
| GCP #10 | 4381084.8509 | 5486356.1106 | 4381084.8499 | 5486356.1110 | 0.0011 | -0.0005 | 0.0000 | 0.0000 |
| GCP #11 | 4389716.6917 | 5494355.3616 | 4389716.6890 | 5494355.3585 | 0.0027 | 0.0031 | 0.0000 | 0.0000 |
| GCP #12 | 4404055.1718 | 5493460.2788 | 4404055.1699 | 5493460.2802 | 0.0019 | -0.0015 | 0.0000 | 0.0000 |
| GCP #13 | 4389188.2187 | 5462506.7543 | 4389188.2099 | 5462506.7797 | 0.0088 | -0.0254 | 0.0001 | 0.0006 |
| GCP #14 | 4403628.3387 | 5464898.7354 | 4403628.3513 | 5464898.7433 | -0.0126 | -0.0078 | 0.0002 | 0.0001 |
| GCP #15 | 4395661.0595 | 5466449.3683 | 4395661.0613 | 5466449.3700 | -0.0019 | -0.0017 | 0.0000 | 0.0000 |
| GCP #16 | 4405341.5190 | 5478796.2792 | 4405341.5210 | 5478796.2791 | -0.0020 | 0.0001 | 0.0000 | 0.0000 |
| GCP #17 | 4398549.4678 | 5490630.0609 | 4398549.4696 | 5490630.0607 | -0.0017 | 0.0002 | 0.0000 | 0.0000 |
| GCP #18 | 4401216.8360 | 5471742.9270 | 4401216.8361 | 5471742.9339 | -0.0002 | -0.0069 | 0.0000 | 0.0000 |
| GCP #19 | 4386578.0997 | 5478908.9378 | 4386578.1099 | 5478908.9498 | -0.0102 | -0.0120 | 0.0001 | 0.0001 |
| GCP #20 | 4389144.7108 | 5486049.5994 | 4389144.7103 | 5486049.5999 | 0.0005 | -0.0005 | 0.0000 | 0.0000 |
| GCP #21 | 4398928.4737 | 5483009.1745 | 4398928.1902 | 5483009.3399 | 0.2835 | -0.1654 | 0.0804 | 0.0274 |
| GCP #22 | 4390920.9242 | 5470050.0659 | 4390920.9220 | 5470050.0699 | 0.0022 | -0.0040 | 0.0000 | 0.0000 |
| GCP #23 | 4380104.3207 | 5476738.2906 | 4380104.2991 | 5476738.3466 | 0.0216 | -0.0560 | 0.0005 | 0.0031 |
| GCP #24 | 4394680.9617 | 5474301.6969 | 4394680.9603 | 5474301.7099 | 0.0014 | -0.0131 | 0.0000 | 0.0002 |
| GCP #25 | 4384025.6911 | 5463490.2707 | 4384025.7096 | 5463490.2802 | -0.0185 | -0.0095 | 0.0003 | 0.0001 |

| | | | |
|---|---|---|---|
| | | Σ | 0.0836 | 0.0366 |
| RMS X | 0.057829751 | | |
| RMS Y | 0.038261889 | Σ (ΔX²ΔY²) | 0.120206306 |
| | | {Σ (ΔX²ΔY²)} / (ΣGCP's-1) | 0.005008596 |
| | | Genauigkeit [m] | 0.070771435 |

| GCP-ID | X-Satellitenbild | Y-Satellitenbild | X-Referenz | Y-Referenz | Δ X-Sat X-Referenz | Δ Y-Sat Y-Referenz | ΔX² | ΔY² |
|---|---|---|---|---|---|---|---|---|
| GCP #1 | 2559790.9554 | 5639937.6952 | 2559790.9455 | 5639937.5677 | 0.0098 | 0.1274 | 0.0001 | 0.0162 |
| GCP #2 | 2556467.8777 | 5631383.1250 | 2556467.5660 | 5631383.2887 | 0.3117 | -0.1638 | 0.0971 | 0.0268 |
| GCP #3 | 2563388.2503 | 5625756.8380 | 2563388.2581 | 5625756.8412 | -0.0078 | -0.0032 | 0.0001 | 0.0000 |
| GCP #4 | 2560261.5858 | 5615892.6063 | 2560261.5832 | 5615892.6080 | 0.0026 | -0.0017 | 0.0000 | 0.0000 |
| GCP #5 | 2553366.8300 | 5639090.0713 | 2553367.0788 | 5639090.1034 | -0.2488 | -0.0321 | 0.0619 | 0.0010 |
| GCP #6 | 2549963.4684 | 5618659.7525 | 2549963.4705 | 5618659.7486 | -0.0021 | 0.0039 | 0.0000 | 0.0000 |
| GCP #7 | 2543954.5223 | 5627452.6892 | 2543954.5230 | 5627452.6874 | -0.0007 | 0.0018 | 0.0000 | 0.0000 |
| GCP #8 | 2544359.3189 | 5637853.1928 | 2544359.3149 | 5637853.1924 | 0.0040 | 0.0004 | 0.0000 | 0.0000 |
| GCP #9 | 2544276.4827 | 5615614.4394 | 2544276.4846 | 5615614.4450 | -0.0019 | -0.0056 | 0.0000 | 0.0000 |
| GCP #10 | 2547231.6314 | 5634453.9077 | 2547231.6315 | 5634453.9082 | -0.0002 | -0.0005 | 0.0000 | 0.0000 |
| GCP #11 | 2564639.6265 | 5636561.7160 | 2564639.6493 | 5636561.7044 | -0.0228 | 0.0115 | 0.0005 | 0.0001 |
| GCP #12 | 2554276.7417 | 5616695.2562 | 2554276.7363 | 5616695.2149 | 0.0054 | 0.0413 | 0.0000 | 0.0017 |
| GCP #13 | 2559439.7688 | 5620415.4124 | 2559439.7790 | 5620415.4133 | -0.0102 | -0.0008 | 0.0001 | 0.0000 |
| GCP #14 | 2546761.5215 | 5621990.5059 | 2546761.5197 | 5621990.5096 | 0.0018 | -0.0037 | 0.0000 | 0.0000 |
| GCP #15 | 2563274.6665 | 5630728.4868 | 2563274.6539 | 5630728.5042 | 0.0126 | -0.0174 | 0.0002 | 0.0003 |
| GCP #16 | 2553862.8901 | 5634950.4936 | 2553862.9324 | 5634950.4611 | -0.0423 | 0.0325 | 0.0018 | 0.0011 |
| GCP #17 | 2554544.1173 | 5620694.6639 | 2554544.1201 | 5620694.6901 | -0.0028 | -0.0262 | 0.0000 | 0.0007 |
| GCP #18 | 2551257.8958 | 5624998.8765 | 2551257.9048 | 5624998.8821 | -0.0089 | -0.0057 | 0.0001 | 0.0000 |
| GCP #19 | 2557808.7627 | 5624204.4941 | 2557808.7612 | 5624204.5090 | 0.0015 | -0.0149 | 0.0000 | 0.0002 |
| GCP #20 | 2544055.8302 | 5631579.7368 | 2544055.8190 | 5631579.7306 | 0.0112 | 0.0062 | 0.0001 | 0.0000 |
| GCP #21 | 2548406.4152 | 5628893.3174 | 2548406.4247 | 5628893.3240 | -0.0095 | -0.0066 | 0.0001 | 0.0000 |
| GCP #22 | 2554834.2546 | 5626651.9677 | 2554834.2451 | 5626651.9423 | 0.0095 | 0.0254 | 0.0001 | 0.0006 |
| GCP #23 | 2552538.6978 | 5629762.0162 | 2552538.8067 | 5629762.1520 | -0.1088 | -0.1358 | 0.0118 | 0.0184 |
| GCP #24 | 2557309.4023 | 5635645.1928 | 2557309.3990 | 5635645.1017 | 0.0033 | 0.0911 | 0.0000 | 0.0083 |
| GCP #25 | 2549066.4539 | 5639129.9821 | 2549066.5724 | 5639129.9560 | -0.1185 | 0.0261 | 0.0140 | 0.0007 |

| | | | |
|---|---|---|---|
| | | Σ | 0.1882 | 0.0765 |

| | |
|---|---|
| RMS X | 0.086753696 |
| RMS Y | 0.055305954 |

| | |
|---|---|
| Σ (ΔX²ΔY²) | 0.264623809 |
| {Σ (ΔX²ΔY²)} / (ΣGCP's-1) | 0.011025992 |
| Genauigkeit [m] | 0.105004724 |

| | Ortho ID | Acquisition date | Across track incidence angle [deg] | Coordinate system and zone | Site name | Environment |
|---|---|---|---|---|---|---|
| WEIL1 | 2009-04-21T111505_RE3_3A-NAC_953000_38645_GK2 | 21/04/2009 | 7.6 | Gauß-Krueger 2 | WEIL | 80% rural / 20% urban |
| MFRA1 | 2009-06-13T110742_RE4_3A-NAC_1214946_44695_GK | 13/06/2009 | 5.2 | Gauß-Krueger 4 | MFRA | 80% rural / 20% urban |
| MFRA2 | 2009-06-13T110746_RE4_3A-NAC_1136205_44574_GK | 13/06/2009 | 5.7 | Gauß-Krueger 4 | MFRA | 80% rural / 20% urban |

| | Relief characteristics | Elevation range [m] | Max distance from the central meridian [km] | Min distance from the central meridian [km] | Mean angular distance from the central meridian ($\Delta\lambda$) | Mean angular distance from the equator ($\Delta\phi$) |
|---|---|---|---|---|---|---|
| WEIL1 | gently sloping topography | 50-200 | 69 | 43 | 0°49'13" | 50°46'57" |
| MFRA1 | hilly topography with relative heights up to 150m | 300-480 | 121 | 97 | 1°31'31" | 49°29'56" |
| MFRA2 | hilly topography with relative heights up to 150m | 300-480 | 122 | 98 | 1°31'54" | 49°16'59" |

| | ECQ EFTAS RMSE_X (E) [m] | ECQ EFTAS RMSE_Y (N) [m] | ECQ EFTAS RMSE_X (E) after shift elimination [m] | ECQ EFTAS RMSE_Y (N) after shift elimination [m] | ECQ CID RMSE_X (E) [m] | ECQ CID RMSE_Y (N) [m] | ECQ CID RMSE_X (E) after shift elimination [m] | ECQ CID RMSE_Y (N) after shift elimination [m] |
|---|---|---|---|---|---|---|---|---|
| WEIL1 | 1.83 | 1.82 | 1.80 | 1.71 | 2.58 | 2.74 | 2.58 | 2.69 |
| MFRA1 | 5.02 | 7.04 | 5.02 | 2.36 | 5.14 | 2.68 | 5.13 | 2.67 |
| MFRA2 | 4.44 | 9.77 | 4.25 | 2.70 | 14.26 | 9.63 | 4.02 | 1.74 |

**Appendix 8: Metadata summary and quality control results for the three tested enhanced RapidEye level 3A tiles (WEIL1, MFRA1, MFRA2)**

**UTM**

| | 2009-06-13T110739_RE4_3A-NAC_**1214946_44695**_GK | | 2009-06-13T110739_RE4_3A-NAC_**1136205_44574**_GK | | Difference | |
|---|---|---|---|---|---|---|
| | X Measured [m] | Y Measured [m] | X Measured [m] | Y Measured [m] | X [m] | Y [m] |
| CP#239 | 598400.043 | 5471885.210 | 598414.741 | 5471880.311 | -14.698 | 4.899 |
| CP#240 | 599884.749 | 5472005.312 | 599900.005 | 5472000.015 | -15.256 | 5.297 |
| CP#241 | 604879.651 | 5471875.048 | 604894.760 | 5471864.976 | -15.109 | 10.072 |
| CP#242 | 607889.736 | 5471929.946 | 607904.658 | 5471920.233 | -14.922 | 9.713 |
| CP#243 | 609539.843 | 5472170.297 | 609554.957 | 5472159.992 | -15.114 | 10.305 |
| CP#244 | 611689.977 | 5471960.130 | 611705.147 | 5471950.290 | -15.170 | 9.840 |
| CP#245 | 614064.831 | 5471804.746 | 614080.021 | 5471795.153 | -15.190 | 9.593 |
| CP#246 | 615869.867 | 5471895.080 | 615885.020 | 5471885.073 | -15.153 | 10.007 |
| CP#247 | 618374.658 | 5471815.003 | 618389.537 | 5471804.968 | -14.879 | 10.035 |
| CP#248 | 619840.087 | 5471595.162 | 619855.159 | 5471585.354 | -15.072 | 9.808 |
| | | | | **Mean** | **-15.06** | **8.96** |
| | | | | **Standard deviation** | **0.17** | **2.05** |

**Gauss-Krueger**

| | 2009-06-13T110739_RE4_3A-NAC_**1214946_44695**_GK | | 2009-06-13T110739_RE4_3A-NAC_**1136205_44574**_GK | | Difference | |
|---|---|---|---|---|---|---|
| | X Measured [m] | Y Measured [m] | X Measured [m] | Y Measured [m] | X [m] | Y [m] |
| CP#219 | 4380017.396 | 5474002.260 | 4380031.872 | 5473999.509 | -14.476 | 2.751 |
| CP#220 | 4382849.121 | 5473913.967 | 4382863.207 | 5473906.484 | -14.086 | 7.483 |
| CP#221 | 4387374.224 | 5474324.804 | 4387389.195 | 5474316.978 | -14.971 | 7.826 |
| CP#222 | 4389456.995 | 5474132.948 | 4389473.004 | 5474129.836 | -16.009 | 3.112 |
| CP#223 | 4391261.196 | 5473669.885 | 4391272.347 | 5473662.303 | -11.151 | 7.582 |
| CP#224 | 4393415.956 | 5473638.507 | 4393426.990 | 5473625.838 | -11.034 | 12.669 |
| CP#225 | 4394222.640 | 5473217.754 | 4394238.570 | 5473210.488 | -15.930 | 7.266 |
| CP#226 | 4396794.714 | 5473207.153 | 4396811.400 | 5473194.792 | -16.686 | 12.361 |
| CP#227 | 4398675.563 | 5473493.270 | 4398687.795 | 5473480.617 | -12.232 | 12.653 |
| CP#228 | 4400643.948 | 5473311.417 | 4400660.997 | 5473298.406 | -17.049 | 13.011 |
| | | | | **Mean** | **-14.36** | **8.67** |
| | | | | **Standard deviation** | **2.22** | **3.88** |

**Appendix 9.1: Shift measurements between MFRA1 and MFRA2 tiles projected in UTM (upper table) and Gauss-Krueger projection (lower table).**

**UTM**

| | 2009-06-13T110739_RE4_3A-NAC_**1136128_44574**_GK | | 2009-06-13T110739_RE4_3A-NAC_**1214946_44695**_GK | | Difference | |
|---|---|---|---|---|---|---|
| | X Measured [m] | Y Measured [m] | X Measured [m] | Y Measured [m] | X [m] | Y [m] |
| CP#249 | 596794.845 | 5495779.849 | 596769.865 | 5495785.087 | -24.980 | 5.238 |
| CP#250 | 599379.420 | 5495779.909 | 599354.418 | 5495785.118 | -25.002 | 5.209 |
| CP#251 | 603344.546 | 5495965.009 | 603319.291 | 5495974.831 | -25.255 | 9.822 |
| CP#252 | 604694.974 | 5496044.803 | 604670.238 | 5496054.781 | -24.736 | 9.978 |
| CP#253 | 607549.766 | 5496370.083 | 607524.709 | 5496380.106 | -25.057 | 10.023 |
| CP#254 | 610654.609 | 5496335.356 | 610629.647 | 5496345.757 | -24.962 | 10.401 |
| CP#255 | 612325.435 | 5496184.963 | 612300.028 | 5496195.039 | -25.407 | 10.076 |
| CP#256 | 614324.702 | 5496029.767 | 614299.477 | 5496040.172 | -25.225 | 10.405 |
| CP#257 | 617154.768 | 5496195.309 | 617129.739 | 5496204.979 | -25.029 | 9.670 |
| CP#258 | 618619.490 | 5495720.483 | 618594.476 | 5495730.357 | -25.014 | 9.874 |
| | | | | **Mean** | **-25.07** | **9.07** |
| | | | | **Standard deviation** | **0.19** | **2.04** |

**Gauss-Krueger**

| | 2009-06-13T110739_RE4_3A-NAC_**1136128_44574**_GK | | 2009-06-13T110739_RE4_3A-NAC_**1214946_44695**_GK | | Difference | |
|---|---|---|---|---|---|---|
| | X Measured [m] | Y Measured [m] | X Measured [m] | Y Measured [m] | X [m] | Y [m] |
| GCP#1 | 4381426.936 | 5498423.769 | 4381399.923 | 5498434.890 | -27.013 | 11.121 |
| CP#200 | 4384387.646 | 5498048.556 | 4384365.278 | 5498065.125 | -22.368 | 16.569 |
| CP#201 | 4387122.799 | 5497711.000 | 4387100.743 | 5497722.396 | -22.056 | 11.396 |
| CP#202 | 4388000.421 | 5497960.183 | 4387973.429 | 5497971.547 | -26.992 | 11.364 |
| CP#203 | 4392592.919 | 5497502.791 | 4392567.209 | 5497514.335 | -25.710 | 11.544 |
| CP#204 | 4393844.442 | 5497633.565 | 4393819.602 | 5497644.905 | -24.840 | 11.340 |
| CP#205 | 4394334.499 | 5497243.793 | 4394305.057 | 5497254.588 | -29.442 | 10.795 |
| CP#206 | 4395639.151 | 5497793.910 | 4395614.155 | 5497805.020 | -24.996 | 11.110 |
| CP#207 | 4400424.127 | 5497607.343 | 4400398.699 | 5497618.427 | -25.428 | 11.084 |
| CP#208 | 4401853.135 | 5497180.945 | 4401828.693 | 5497191.932 | -24.442 | 10.987 |
| | | | | **Mean** | **-25.33** | **11.73** |
| | | | | **Standard deviation** | **2.19** | **1.71** |

**Appendix 9.2: Shift measurements between MFRA0 and MFRA1 tiles projected in UTM (upper table) and Gauss-Krueger projection (lower table).**

European Union

**EUR 24132 EN – Joint Research Centre – Institute for the Protection and Security of the Citizen**
Title: Analysis of the geometric quality of the LPIS-based RapidEye level 3A product
Author(s): Joanna Krystyna Nowak Da Costa, Piotr Andrzej Tokarczyk
Luxembourg: Office for Official Publications of the European Communities
2009 – 47 pp. – 21.0 x 29.7 cm
EUR – Scientific and Technical Research series – ISSN 1018-5593
ISBN 978-92-79-14625-1
DOI 10.2788/52547

**Abstract**
This report describes the geometric image quality of the LPIS-based RapidEye level 3A product in the context of the Common Agriculture Policy (CAP) Control with Remote Sensing (CwRS) Programme. This product is similar to the RE standard level 3A product, but the standard RapidEye planimetric auxiliary data is replaced with a set of ground control points derived from the LPIS vector data.
Based on the current analysis there are two issues that most likely driving the differences in the geometric quality of the provided tiles: the heterogonous quality of the input height data and a low polynomial order for reprojection to the Gauss-Krueger. In order to comprehensively verify these hypotheses, the quality analysis must be repeated.
Based on the limited RapidEye sample images, the accuracy of the LPIS-based RapidEye level 3A products is within the RE product specifications accuracy (1-D RMSE of 6.5m) provided the shift elimination based on the set of well-distributed ground control points.

The mission of the JRC is to provide customer-driven scientific and technical support for the conception, development, implementation and monitoring of EU policies. As a service of the European Commission, the JRC functions as a reference centre of science and technology for the Union. Close to the policy-making process, it serves the common interest of the Member States, while being independent of special interests, whether private or national.

JRC
EUROPEAN COMMISSION

LB- NA- 24132- EN-C

ISBN 978-92-79-14625-1


Publications Office
Publications.europa.eu